ELECTRO-SPARK DEPOSITION TECHNOLOGY

Roger N. Johnson

Battelle, Pacific Northwest National Laboratory
P.O. Box 999, K3-59
Richland, Washington 99352

ABSTRACT

Electro-Spark Deposition (ESD) is a micro-welding process that uses short duration, high-current electrical pulses to deposit or alloy a consumable electrode material onto a metallic substrate. The ESD process was developed to produce coatings for use in severe environments where most other coatings fail. Because of the exceptional damage resistance of these coatings, and the versatility of the process to apply a wide variety of alloys, intermetallics, and cermets to metal surfaces, the ESD process has been designated as one of the enabling technologies for advanced energy systems. Protective coatings will be critical to the life and economy of the advanced fossil energy systems as the higher temperatures and corrosive environments exceed the limits of known structural materials to accommodate the service conditions.

Developments include producing iron aluminide-based coatings with triple the corrosion resistance of the best previous Fe_3Al coatings, coatings with refractory metal diffusion barriers and multi layer coatings for achieving functionally gradient properties between the substrate and the surface. A new development is the demonstration of advanced aluminide-based ESD coatings for erosion and wear applications. One of the most significant breakthroughs to occur in the last dozen years is the discovery of a process regime that yields an order of magnitude increase in deposition rates and achievable coating thicknesses. Achieving this regime has required the development of advanced ESD electronic capabilities. Development is now focused on further improvements in deposition rates, system reliability when operating at process extremes, and economic competitiveness.

Technology transfer activities are a significant portion of the ESD program effort. Notable successes now include the start-up of two new businesses to commercialize the ESD technology, the incorporation of the process into the operations of two major gas turbine manufacturers, major new applications in gas turbine and steam turbine protection and repair, and in military, medical, metal-working, and recreational equipment applications.

INTRODUCTION

The objective of this program is to develop an advanced coating process capable of meeting the surface treatment requirements for the next and future generations of advanced fossil energy systems. This includes the development and testing of new materials and coatings with the ability to operate in severe environments beyond current materials limits, and to provide improvements in performance, durability and cost effectiveness for both new and existing power systems. Ultimately new materials performance limits can enable new systems concepts.

A corollary objective is to further advance the Electro-Spark Deposition (ESD) technology and equipment, and to develop broad commercial applications through technology transfer activities.

Just as high performance jet engines would not be possible today without protective metallurgical coatings, so also does the next generation of high efficiency energy systems depend on protective coatings to survive the necessarily higher temperatures and more corrosive environments. The ESD coating process has been designated as one of the enabling technologies for such future systems. One of the reasons for this is that the exceptional structure produced in these metallurgically-bonded coatings makes them virtually immune to damage or spalling under severe service conditions and temperatures that destroy most other coatings. Additional attractions are that the process is portable (allowing coatings or surface treatments to be performed in the field), environmentally benign (creates no noxious wastes, fumes or effluents), and highly cost-effective.

BACKGROUND

The ESD process was developed to provide exceptionally robust coatings for use in nuclear reactor environments when all other commercially available coatings either failed to survive the severe conditions or failed to meet the performance requirements. The Fossil

Energy Program leveraged on that success to begin further developing the ESD process, coatings and applications to meet the demands of advanced fossil energy systems. Electro-spark deposition is a pulsed-arc micro-welding process that uses short-duration, high-current electrical pulses to weld a consumable electrode material to a metallic substrate. The short duration of the electrical pulse allows an extremely rapid solidification of the deposited material and results in an extremely fine-grained, homogeneous coating that may be amorphous for some materials. The microstructures thus produced are believed to be responsible for the superior corrosion and wear performance usually exhibited by the ESD coatings when compared to similar coatings applied by other processes.

The ESD process is one of the few methods available by which a fused, metallurgically-bonded coating can be applied with such a low total heat input that the bulk substrate material remains at or near ambient temperatures. This eliminates thermal distortions or changes in metallurgical structure of the substrate. Not only is the coating metallurgically-bonded, but it exhibits a functional gradient in composition and properties through the coating thickness. This eliminates the "metallurgical notch" associated with coatings that have an abrupt property change at the coating/substrate interface. The metallurgical bond and the elimination of this notch makes ESD coatings inherently more resistant to damage and spalling than the mechanically-bonded coatings produced by most other low-heat-input processes such as detonation gun, plasma spray, electro-chemical plating, etc. Nearly any electrically-conductive metal, alloy, intermetallic, or cermet can be applied by ESD to metal substrates.

Further background information on the ESD process is provided in Ref. 1 and 2.

DISCUSSION OF PRIOR ACTIVITIES

Chromium Carbide Experiments

ESD coatings usually show lower corrosion rates in most environments than the same material would in either bulk form or as a coating applied by other processes.[3] The superior performance of the ESD deposit is attributed to the fine-grained, nearly amorphous nano-structure inherent to the ESD coatings that is not normally achieved in other coating technologies.

In tests at Argonne National Laboratory (ANL), a nano-structured ESD chromium carbide-15% Ni coating showed (unexpectedly) four times better sulfidation resistance than Type 310 stainless steel at 875 C.[4] Normally, this composition would not be expected to perform that well because of the strong susceptibility of a nickel matrix to sulfidation attack. Again, the near amorphous structure is believed to be a major factor in the corrosion resistance. This observation is in agreement with other Fossil Energy Program work that indicates one mechanism of improving lifetimes of protective oxide films and scales is to maintain as fine a grain structure as possible.[5]

Iron Aluminide Coating Development

One of the most significant advances in ESD coatings for use in sulfidation environments has been the successful development of Fe_3Al as a coating material. Oak Ridge National Laboratory (ORNL) has demonstrated the exceptional corrosion properties of Fe_3Al in bulk form, but alloying to achieve acceptable mechanical properties while maintaining optimum corrosion resistance appears to be a challenge. One alternative is to use the most corrosion-resistant compositions as coatings. These iron aluminide compositions have proved to be nearly ideal for use in the ESD process. Consistent, defect-free coatings over 100 μm can be applied rapidly, uniformly and economically.

Sulfidation corrosion tests showed that weld-dilution effects with the substrate

material must be controlled to keep the aluminum content at the surface above the threshold 12% Al that appears to be necessary for good sulfidation resistance.[6,7] Three methods for increasing the aluminum content ultimately were tried. In the first, a simple process of alloying of the surface by ESD using an aluminum electrode was successful in producing aluminum enrichment, but the resulting structure was excessively cracked.[8] The second technique involved a preliminary coating (by ESD) of the substrate with a refractory metal, such as niobium or molybdenum. The higher melting material successfully served as a barrier to diffusion of the substrate material into the coating during subsequent ESD coating. This resulted in achieving a surface composition of good integrity undiluted with substrate elements, and doubled the corrosion resistance.[7] The third method was to use an electrode with a significantly higher Al content, such as FeAl.[9] This material also proved to be well-suited to the ESD process and resulted in the best corrosion performance achieved to date for coatings in coal combustion and coal gasification environments.[10]

DISCUSSION OF CURRENT ACTIVITIES

Process and Equipment Development

The advantages of the Electro-Spark Deposition process, summarized earlier, make it highly attractive for many advanced energy system applications, especially where it is often the only practical surface modification with adequate robustness to survive in severe service conditions. For applications involving limited areas of treatment, the ESD process also can be among the least expensive surface treatments available. But one of the process limitations is the relatively slow deposition rate for large areas compared to higher energy processes, such as thermal spray, conventional welding, diffusion coating, etc. The ESD's lower energy input that produces the unique nano-structures, attractive properties and low substrate effects also restricts the deposition rate.

A major thrust of current activities has been to identify methods of significantly increasing deposition rates while maintaining the properties and structure typical of the ESD

coatings. Achievement of higher rates will increase the number of fossil energy and other applications where ESD can be considered economically attractive.

Exploration of ESD welding parameters at and near the limits of our power supply capabilities has revealed a distinctly different deposition regime for some materials. When this regime is achieved, deposition rates increase by as much as an order of magnitude. The coating thickness limitations usually inherent to most ESD deposits appear to be eliminated. Whereas 100 microns (0.004 in) is normally considered a practical maximum under most circumstances, we have achieved coatings as thick as 1 mm (0.04 in).

This discovery sparked an effort to develop a next generation power supply that can consistently exploit this regime of deposition parameters without damage to the supply or its reliability. An improved prototype ESD power supply was developed that so far has improved deposition rates by 300 to 500% for most materials.

In addition to increased deposition rates, other improvements achieved include:

a) increased stability in the higher power regimes,

b) improved safety circuits for shock protection

c) improved computer controls, including replacement of chips to give non-volatile memory for key functions.

The power supply, of course, is only one element of the ESD system. Another important part is the device used to control the electrode-to-substrate motion and geometry. This is accomplished in the applicator head and controls, and typically has involved mounting servo-controlled motors directly on the applicator. A new design for an applicator that relocates the motor away from the head has been completed and fabrication of the prototype is in progress. The benefits expected are reduced mass of applicator, less operator fatigue for manual coating operations, and less stress on automated machine components in computer-controlled coating applications.

These advances mark the greatest improvements in the ESD technology in the past decade. Further improvements appear possible as more advanced and robust components capable of meeting our particular current and pulse duration requirements become commercially available.

Materials Development and Testing

Coatings of iron aluminides were successfully completed using a new, experimental (and less expensive) electrode fabricated by Stoody Co. The new electrode is formed by drawing or swaging an iron tube on to an aluminum core to produce an average cross sectional composition equivalent to the alloy composition desired in the final deposit. This avoids making a special heat of the alloy and then forming it into electrodes. Preliminary evaluations of the deposits show that the coatings are of equivalent quality to those made from pre-alloyed electrodes.

The first series of wear and erosion tests on candidate ESD coatings were completed. The coatings included iron aluminides, nickel aluminides, and titanium aluminides containing 0 to 10 wt.% TiB_2. The erosion tests (ASTM G-76) showed Ti_3Al to have the lowest erosion rate (0.13 mg/g of Al_2O_3 erodent) of the pure aluminide coatings, Ni_3Al to have the highest rate (0.40 mg/g), and Fe_3Al an intermediate erosion rate (0.30 mg/g). As expected, TiB_2 additions were beneficial in improving both wear and erosion resistance. The lowest erosion rate was achieved by an ESD coating of TiAl-10 wt.% TiB_2 (0.095 mg/g). Low stress abrasion tests (ASTM 1044) resulted in a similar ranking of the coatings. Further wear and erosion tests will be conducted on iron aluminide-base coatings containing TiC and TiB_2 when suitable electrodes being developed become available.

Technology Transfer Highlights

ESD coatings are seeing increasing use in fossil-fueled gas and steam turbine applications. Two major gas turbine manufacturers have qualified ESD coatings for use in several engine components and a steam turbine manufacturer has ESD coatings in long-term qualification tests.

The most recent ESD qualification to be placed in production involves the deposition of wear-resistant carbides to turbine blade tips for wear against abradable seals.

Such seals are critical to improved performance and fuel efficiency. The ESD coatings not only out-perform all previously used coatings, but they can be applied without affecting the single crystal structure of the advanced turbine blades used. Other turbine power plant ESD applications include:

a) build-up of high-value worn or mis-machined parts to acceptable tolerances,

b) Pt coating of blades on selected areas for subsequent incorporation into aluminide diffusion coatings,

c) repair of damaged aluminide diffusion coatings,

d) pre-placement of braze alloys for precision assembly of complex components,

e) coating of high-wear contact points in turbine assemblies,

f) elimination of stress-corrosion-cracking problems by surface treatment of critical high stress areas of components with special corrosion-resistant alloys.

Other successful applications, recently commercialized, where ESD coatings have out-performed all other surface treatments evaluated in combined corrosion and wear environments include:

a) coating of dies and cutter plates used in the extrusion and cutting of processed food products at 177 C (350 F) and 17.3 MPa (2500 psi),

b) pulp and paper mill plug screws and barrel extruders, where service lives have been increased from six months to two years at last report, and are still in service.

c) surface modifications to increase sparking resistance of components used in potentially explosive atmospheres.

ESD coatings now in test for severe service applications include: a) digging tools to be used by NASA's Mars Lander, b) cutters for multi-material chipping operations in recycling plants, c) tools user in the machining and metal working of titanium alloys, and d) seals and bearings used on tri-clone bits in deep well drilling for oil production.

REFERENCES

1. R.N. Johnson, "Principals and Applications of Electro-Spark Deposition," *Surface Modification Technologies*, T.S. Sudarshan and D.G. Bhat, eds., The Metallurgical Society, January 1988, p. 189-213.

2. R.N. Johnson, "Electro-Spark Deposited Coatings for High Temperature Wear and Corrosion Applications," *Elevated Temperature Coatings: Science and Technology I*, N. B. Dahotre, J.M. Hampikian, and J.J. Stiglich, eds., The Metallurgical Society, October 1994, p. 265-277.

3. R.N. Johnson, "Coatings for Fast Breeder Reactors," in *Metallurgical Coatings*, Elsevier Sequoia, S.A., New York, 1984, p. 31-47.

4. K. Natesan and R.N. Johnson, "Corrosion Resistance of Chromium Carbide Coatings in Oxygen-Sulfur Environments," *Surface and Coatings Technology*, Vol. 33, 1987, p. 341-351.

5. I.G. Wright and J.A. Colwell, "A Review of the Effects of Micro-Alloying Constituents on the Formation and Breakdown of Protective Oxide Scales on High Temperature Alloys at Temperatures Below 700 C," ORNL/Sub/86-57444/01, September 1989.

6. K. Natesan and R.N. Johnson, "Corrosion Performance of Fe-Cr-Al and Fe Aluminide Alloys in Complex Gas Environments," *Heat-Resistant Materials II - 2nd Int. Conf.*, ASM Int., 1995, p.591-600.

7. K. Natesan and R.N. Johnson, "Development of Coatings with Improved Corrosion Resistance in Sulfur-Containing Environments," *Surface and Coatings Technology*, Vol. 3/44, 1990, p. 821-835.

8. R.N. Johnson, "Electro-Spark Deposited Coatings for Fossil Energy Environments," in *Proceedings of the Seventh Annual Conference on Fossil Energy Materials*, ORNL/FMP-93/1, July 1993, p.289-295.

9. R.N. Johnson, "Electro-Spark Deposited Coatings for Protection of Materials," in *Proceedings of the Ninth Annual Conference on Fossil Energy Materials*, ORNL/FMP-95-1, August 1995, p. 407-413.

10. R. N. Johnson, "Electro-Spark Deposition Technology", in *Proceedings of the Tenth Annual Conference on Fossil Energy Materials,* ORNL/FMP-96/1, August 1996, p. 429-437.

INVESTIGATION OF AUSTENITIC ALLOYS FOR ADVANCED HEAT RECOVERY AND HOT-GAS CLEANUP SYSTEMS

R. W. Swindeman

Oak Ridge National Laboratory
P.O. Box 2008
Oak Ridge, TN 37831

ABSTRACT

Materials properties were collected for the design and construction of structural components for use in advanced heat recovery and hot gas cleanup systems. Alloys systems included 9Cr-1Mo-V steel, modified 316 stainless steel, modified type 310 stainless steel, modified 20Cr-25Ni-Nb stainless steel, and modified alloy 800. Experimental work was undertaken to expand the databases for potentially useful alloys. Types of testing included creep, stress-rupture, creep-crack growth, fatigue, and post-exposure short-time tensile tests. Because of the interest in relatively inexpensive alloys for service at 700°C and higher, research emphasis was placed on a modified type 310 stainless steel and a modified 20Cr-25Ni-Nb stainless steel. Both steels were found to have useful strength to 925°C with good weldability and ductility.

INTRODUCTION

The objective of the research is to provide databases and design criteria to assist in the selection of optimum alloys for construction of components needed to contain process streams in advanced heat recovery and hot gas cleanup systems. Typical components include: steam line piping and superheater tubing for low emission boilers (600 to 700°C), heat exchanger tubing for advanced steam (650 to 800°C), foil materials for recuperators on advanced turbine systems (700 to 750°C), and tubesheets, plenums, liners, and blowback systems for hot gas cleanup vessels (850 to 1000°C).

STEELS FOR LOW EMISSION BOILERS

Alloys such as vanadium-modified 2 1/4 Cr-1 Mo, 2 1/4Cr-1.5W, 9Cr-1Mo, 9Cr-1.5W and 12Cr-1.5W steels are candidates for the construction of piping, headers, and tubing in the low emission boiler (LEB) project supported by the Pittsburgh Energy Technology Center. However, these classes of steels exhibit a complex metallurgical constitutions that are not fully understood, and concerns exist about long-term embrittlement due to Laves

phase precipitation, degradation of weldments due to cavitation cracking, and susceptibility to creep-fatigue damage. Methods for on-line damage assessment are needed as an assurance against component failures. To assist the LEB project contractors in addressing these issues, damage accumulation mechanisms in 9Cr-1Mo-V steel are being studied. These studies involve the continuation of long-time creep testing on aged 9Cr-1Mo-V steel, the examination of correlation methods to relate mechanical behavior time-temperature-stress history, studies of thick-section weldment behavior, and the assessment of damage in service-exposed materials. Damage studies are being undertaken on T91 tubing removed from the superheater of a power boiler after sixteen years of service. The tubing included dissimilar metal welds between T91, T22, and 321 stainless steel. Metallurgical studies showed minor cracking at the joints in both the 321 stainless steel and T91. The Gr91 tubing retained good strength and ductility. When compared on the basis of the Larson Miller parameter, short-time stress-rupture data for T91 fell near the bottom of the scatterband for unexposed material. Data are plotted in Fig. 1. Such behavior was judged to be typical.

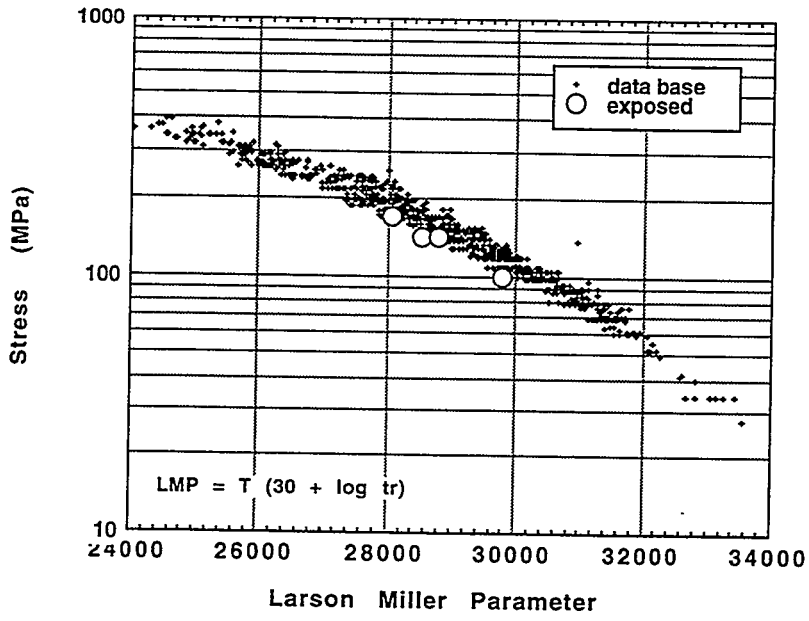

Fig. 1. Comparison of stress-rupture data for service exposed 9Cr-1Mo-V steel to the Larson-Miller scatterband for unexposed material.

Additional studies are needed to examine the performance heavy section weldments in the advanced ferritic alloys. Some welds in the T91 removed from the TVA boiler showed sign of type-IV cracking, and service failures have already occurred in components that were not properly fabricated. Exploratory fatigue and stress-rupture testing of weld in T91 piping has been completed at ORNL and the propensity for the acceleration of type IV cracking under cyclic stresses has been confirmed. For additional studies, and a heavy-section weld of T91 has been received from an industrial fabricator. Here section size effects on creep ductility and creep crack growth will be examined.

In the LEB, austenitic stainless steels will be used for tubing in the hotter, more corrosive sections of the superheater and reheater. Code-approved (ASME Sect. I) candidate steels include fine-grained 347 stainless steel (347FG), niobium-modified 310 stainless steel (310HCbN SS), and alloy 800H. Commercially available stainless steels for which a suitable database exists include a titanium-zirconium-modified 20Cr-25Ni-Nb stainless steel (NF709), a copper-niobium 18Cr-8Ni stainless steel (ST3Cu), and 17-14CuMo stainless steel (previously code-approved). Experimental alloys tested to long times in mechanical and corrosion probes include the modified 316 stainless steels (HT-UPS steels), modified alloy 800H, and Tantalum modified 310 stainless steel. The code-approved several stabilized grades stainless steels have cracked near welds and cold-formed regions, so Sect. I may impose requirements to re-anneal cold-worked tubing of the 347FG, 310HcbN, and alloy 800H. Further studies of these alloys are needed to establish fabrication guidelines for use in boiler construction of the LRB components. Also, further studies are needed to examine issues related to dissimilar metal welds between the advanced stainless steels and new ferritic alloys such as T23, T92, and T92. Under a CRADA with ABB-Combustion Engineering, work was begun to examine cold work effects in austenitic stainless steels. It was observed that the understabilized grades of steels, such as the HT-UPS alloys developed at ORNL, benefitted from cold work to levels of at least 10%. This was partly due to the stability of the microstructure and the resistance of the HT-UPS steels to grain-boundary creep cracking. A specimen examined after 60,000 h of creep at 700°C and 100 MPa was found to have a stable microstructure and no cavitation. The testing of the cold-worked stabilized grades has begun.

Welds in the advanced austenitic stainless steels are being examined in long-time testing. Both autogenous welds and filler metal welds are being investigated to further establish whether stress reduction factors will be needed for some types of weldments. Testing of some weldments has exceeded 30,000 hours. Filler metals include 308/CRE, 16-8-2/CRE, alloy 556, and alloy 117.

Of the austenitic stainless steels advanced steels studied to date, the mod. 20Cr-25Ni-Nb stainless steel appeared to have the best overall performance with respect to fabricability, strength, and corrosion resistance. A comparison of the rupture strength of this steel to 347 stainless steel is shown in Fig. 2, and it may be seen that the steel is significantly stronger than 347 stainless steel.

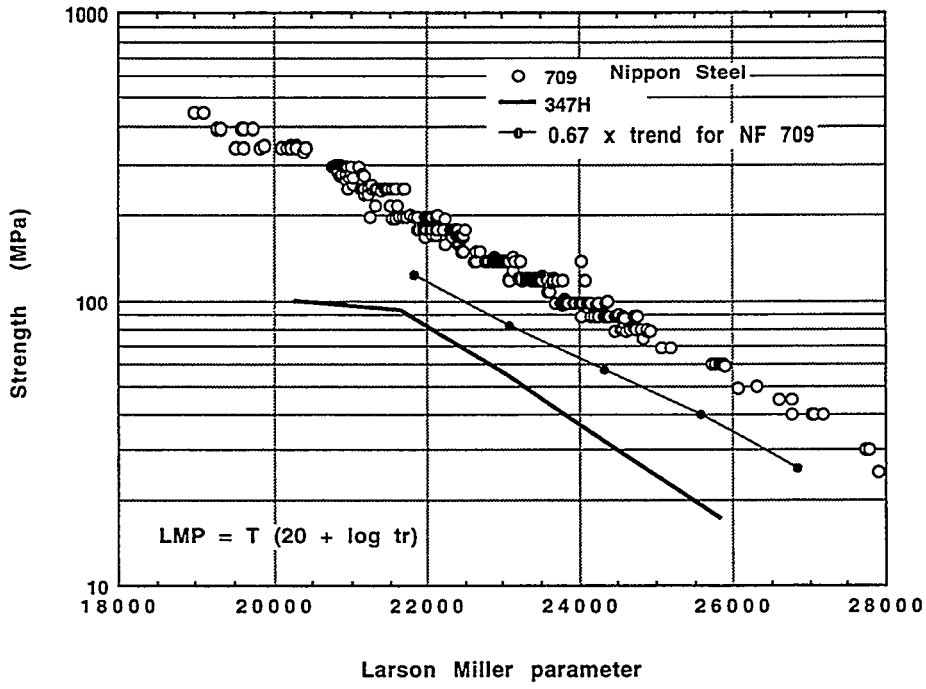

Fig. 2. Comparison of stress-rupture strength for modified 20Cr-25Ni-Nb stainless steel to 347 stainless steel on the basis of the Larson Miller parameter

STEELS FOR ADVANCED HEAT RECOVERY SYSTEMS

Austenitic alloys of interest for advanced heat recovery systems include 347 stainless steel, modified 316 stainless steels, modified 310 stainless steels, and modified 20Cr-25Ni-Nb stainless steels. Current emphasis has been on use of these materials for recuperators. Working on a CRADA with Solar Turbines, Inc., foil materials have been produced at ORNL and are being evaluated in the temperature range of 650 to 730°C. The goal of the development work is to define compositions and fabrication schedules that will produce good creep strength and adequate oxidation resistance in a very fine-grained material for times to beyond 20,000 h. The standard against which the alloy performance is compared is 347 stainless steel now used for service to 600°C. The creep behavior of the materials that have been produced are compared against 347 stainless steel in Fig. 3. Test conditions correspond to 75.8 MPa at 704°C. It is clear that the modified 310 stainless steel and the modified 20Cr-25Ni-Nb steels have significantly better strength for at least 1500 hours. The modified 347 stainless steel has not produced strength equivalent to the standard material.

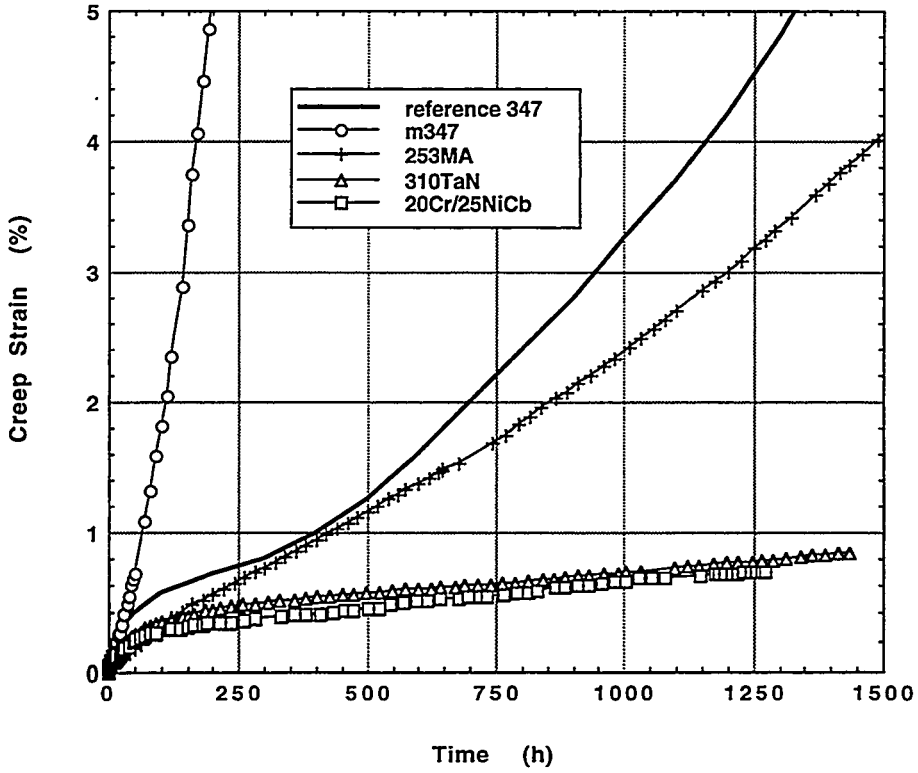

Fig. 3. Comparison of creep curves for candidate recuperator materials at 75.8 MPa and 704°C.

ALLOYS FOR HOT-GAS CLEANUP

Components in several advanced fossil energy systems are expected to experience very high temperatures, and the potential for creep damage, fatigue, thermal-fatigue, and creep-fatigue crack growth are significant. For both "code" alloys and developmental alloys, data for design at very high temperatures are often lacking. For these reasons, exploratory research on creep, creep-fatigue, fatigue, and crack growth of several candidate alloys has been in progress. Earlier work on alloy for hot-gas cleanup involved studies of alloy 333, alloy 556, and alloy 160, which were candidates for use in pressurized fluidized bed (PFBC) hot-gas cleanup systems at temperature above 815°C. More recently, evaluation was completed the heat of alloy 120 that is the tubesheet material in the hot-gas cleanup vessel installed at the Wilsonville PFBC facility. Testing of alloy 120 included creep, creep-crack growth, fatigue, and fatigue-crack growth. Efforts continued to evaluate the performance of modified 310 stainless steel and modified 20Cr-25Ni-Nb stainless steel. Creep testing of the modified 310 stainless steel has exceeded 40,000 h at 871°C, and the material has been found to exhibit good strength and ductility relative to standard 310 stainless steel and alloy 800HT. In Fig. 4. A creep curve is shown for a test at 17.5 MPa and 871°C. Creep strain exceeds 10% at 40,000 h, and a diminishing of the creep rate was observed. This diminishing creep rate is thought to be a manifestation of the influence of the air environment which produces nitriding effects near the free surfaces of the specimen.

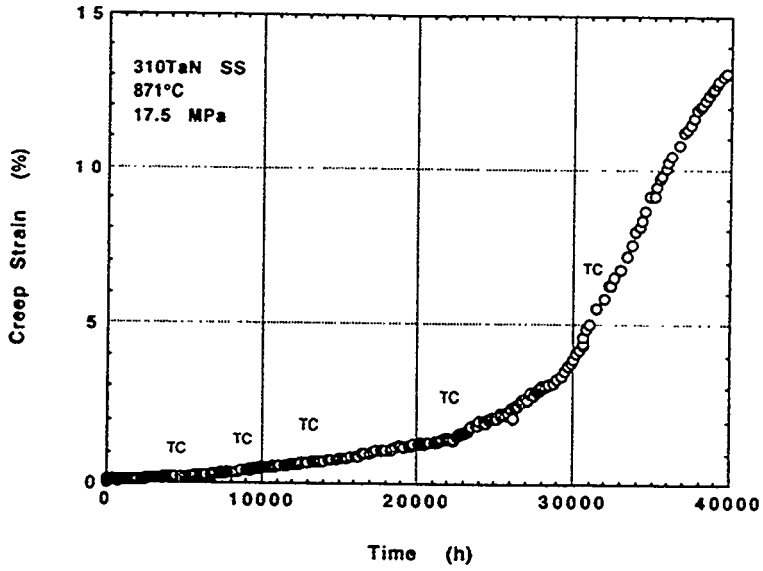

Fig. 4. Long-time creep curve for modified 310 stainless steel at 17.5 MPa and 871°C.

FIRESIDE CORROSION TESTING OF CANDIDATE SUPERHEATER TUBE ALLOYS, COATINGS, AND CLADDINGS - PHASE II

J. L. Blough
W.W. Seitz

Foster Wheeler Development Corporation
12 Peach Tree Hill Road
Livingston, NJ 07039

ABSTRACT

In Phase I a variety of developmental and commercial tubing alloys and claddings were exposed to laboratory fireside corrosion testing simulating a superheater or reheater in a coal-fired boiler. Phase II (in situ testing) has exposed samples of 347 RA-85H, HR3C, 253MA, Fe_3Al + 5Cr, 310 Ta modified, NF 709, 690 clad, and 671 clad for approximately 4,000, 12,000, and 16,000 hours to the actual operating conditions of a 250-MW coal-fired boiler. The samples were assembled on an air-cooled, retractable corrosion probe, the probe was installed in the reheater cavity of the boiler and controlled to the operating metal temperatures of an existing and advanced-cycle coal-fired boiler.

The results will be presented for the preliminary metallurgical examination of the corrosion probe samples after 16,000 hours of exposure. Continued metallurgical and interpretive analysis is still on going.

INTRODUCTION

High-temperature, fireside metal wastage in conventional coal-fired steam generators can be caused by gas-phase oxidation or liquid-phase coal-ash corrosion. Gas-phase oxidation is usually not a problem if tube and support materials are selected for their oxidation resistance at operating temperatures and for spalling, flaking, or other reactions to their environment. Coal-ash corrosion, on the other hand, usually results in accelerated attack and rapid metal wastage—even of stainless steels. The cause of this type of corrosion is generally accepted as the presence of liquid sulfates on the surface of the metal beneath an overlying ash deposit[1-4].

While substantial progress has been achieved through laboratory testing, actual utility service exposures are evidently necessary to verify any conclusions drawn from laboratory testing. A number of important environmental parameters cannot be fully simulated in the laboratory[5]:

- The actual composition of the deposits formed on the tubes is more complex than the composition of the simulated ash.
- The SO_3, formed by heterogeneous reaction on cooled surfaces, is variable.
- Very large temperature gradients occur within the ash deposits.
- The ash and flue gas move past tubes at high velocity; the rate varies with design.
- The composition of the corrosive deposits changes with time.

- Metal and flue-gas temperatures fluctuate.
- Fly-ash erosion removes the protective oxides, exposing a clean surface to fresh ash.

Foster Wheeler Development Corporation (FWDC) has performed a number of literature reviews and recent updates discussing the variables affecting the corrosion mechanism[6-8]. Additionally, Foster Wheeler is conducting two sizable research projects—one a laboratory and in situ field testing at three utilities of commercially available alloys[5,9-14] and this present project (ORNL-FW2)—combining laboratory and field testing to more completely cover the controlling variables for a longer duration[10].

PHASE I RESULTS

In Phase I of this ORNL program, "Fireside Corrosion Testing of Candidate Superheater Tube Alloys, Coatings, and Claddings," 20 commercial and developmental alloys were evaluated[10]. The coupons of the metals were exposed to synthetic coal ash and synthetic flue gases at 650 and 700°C (1202 and 1292°F) for up to 800 hours. The corrosion was evaluated as a function of alkali content in the ash, SO_2 concentration in the gas, and alloy content.

PHASE II CORROSION PROBE TESTING

In this project, the field tests comprise corrosion probe testing, coal characterization, and deposit/corrosion product analysis. The coals have been analyzed to provide fuel characterization, a deposit analysis data bank, and possibly a corrosivity index for predicting corrosivity under various combustion conditions. The equipment and the procedures for this phase have been previously used and perfected at three different utilities for over 3 years of in situ testing at each station.

The utility for test exposures should be burning an aggressive fuel to adequately evaluate the candidate alloys. The coal being burned at Tennessee Valley Authority's (TVA's) Gallatin Station had been previously analyzed, and numerous corrosion indices predicted high corrosivity in addition to the fact that installed T22 and Type 304SS tubing experienced about 7 years of life in the superheaters and reheaters of Units 1 and 2.

Selection of Materials for Corrosion Probes

FWDC tested 20 different materials[10] in the laboratory. Because this quantity was impractical from both an economic and a probe-length standpoint, fewer (the nine listed in Table 1) had to be selected for the field tests. These materials provide a range of compositions and cost for both the commercially available and developmental alloys and claddings.

Field Corrosion Probe Design

The corrosion probes were designed to provide realistic exposures of metal samples to both actual boiler environments and also at the higher anticipated metal temperatures of an advanced plant. The corrosion probes are independent from the main boiler; can be removed without a boiler outage; and have a fail-safe design, one that removes the probe from the boiler if there are any malfunctions. With these features, years of testing will not be compromised with a sudden system overheating.

The probes were exposed for approximately 4000, 12,000, and 16,000 hours. This was accomplished by utilizing two probe test locations. At one test location, the probe was exposed for 15,883 hours. At the other test location, the probe was removed after 4483 hours and a new probe inserted for the remaining 11,348 hours.

Each probe was a 2.56-m (8.4-ft)-long, 60.20-mm (2.37-in.)-OD tube that extended into the furnace for approximately 2.3 m (7.6 ft). Ring samples [38.1 mm (1.5 in.) wide] of the candidate alloys listed in Table 1 were installed at the end of the probe farthest from the furnace wall. The probe was cooled by air that flows in the annular region between the probe tube ID and the tapered inner tube OD. The tapered inner tube was designed to obtain two bands of temperature on the outer surface of the samples. The alloy samples were duplicated in such a manner as to expose each alloy to a temperature in each of the temperature bands [619 to 682°C (1146 to 1260°F) and 682 to 727°C (1260 to 1341°F)].

Table 1. Chemical Composition of Candidate Alloys (wt %)

Alloy	Cr	Ni	Others
Type 347	17-19	9-13	(Nb + Ta) = 10 × C (min.)
85 H	18	15	Al = 1, Si = 3.9
NF 709	20	25	Mo = 1.5, Mn = 1.0, Si = 0.6
690 Clad	30	58	
671 Clad	48	52	
Fe_3Al + 5% Cr	5	—	Al = 17
HR3C	25	20	Nb = 0.4
253 MA	21	11	Si = 1.7
310 Ta modified	25	20	1.5 Ta
800HT	21	32	Al + Ti = 1

Each probe had a retraction mechanism, and three K-type thermocouples in duplicate to monitor the mean tube wall at the beginning and end of each test section group. A 19.95-mm (3/4-in.)-OD thermowell with

sheathed thermocouple was mounted between the corrosion probes to measure flue-gas temperature. Each probe had its own cooling-air control valve.

The control system monitored the selected control thermocouple and modulated the airflow to maintain an average surface metal temperature for each temperature band. The probes retracted automatically if failure of the cooling-air supply system or any other malfunction (instrument signal, power failure, or computer failure) caused the probe temperature to exceed the set limit of 746°C (1375°F) for 2 minutes. FWDC personnel accessed the field computer automatically for probe status and temperature data each morning at 6 a.m. or manually through its modem.

The locations in this plant were chosen because of cavity access and because they best represent the locations for the reheater or superheater outlet on the "Advanced Cycle" unit.

The ideal coal-ash corrosion probe exposure is if only one coal is being burned at the plant. This practice is not common at many utilities; in fact, many are buying coal on the spot market. Gallatin burns a number of eastern high-sulfur coals, mainly Island Creek, Warrior, Dotiri, and Pattiki, which are known to be corrosive and prone to alkali-iron-trisulfate formation. The Borio Index for these coals typically range from 2.0 to 4.1, and the chloride level is 450 to 3000 ppm.

Post-Exposure Analysis

At 4000, 12,000, and 16,000 hours, the probes were removed and sent to FWDC for metallurgical evaluation. The 4,000-hour probe was removed and the analysis reported previously[17]. The 12,000- and 16,000-hour corrosion probes were removed during February 1997 from the reheater cavity of the TVA Gallatin Station Unit 2. The weighted average temperature was calculated for each test section in each of the two probes and is shown in Table 2.

Table 2. Average Exposure Temperature

Test Section	12,000-Hour Probe [°C (°F)]	16,000-Hour Probe [°C (°F)]
1	719-681 (1325-1260)	726-682 (1341-1260)
2	681-623 (1260-1153)	682-619 (1260-1146)

Macroscopic Examination

Both probes were received with a tan deposit on their outer surfaces. The deposits were removed and stored separately for later examination. Two 1/4-in.-long, transverse ring sections were removed from each sample on both probes. One of the ring sections was lightly grit blasted and used for thickness measurements, while the other was mounted for microscopic and SEM/EDX analysis.

Shallow pitting and some surface roughening are evident in some of the samples. The more prominent pitting was noted on samples 1* (RA85H), 5 (HR3C), 11 (RA85H), and 12 (347) from the upper (16,000-hour) probe, and 1 (RA85H) and 4 (RA253MA) in the lower (12,000-hour) probe. Post-exposure wall thickness readings were performed at the 45-, 135-, and 270-degree locations, and wall loss calculated for each sample. [Note: Further microexamination revealed that some of the wall loss in the clad samples 6, 7, 16, and 17 resulted from the oxidation of the inside surface which was a modified LSS (lean 316 stainless steel) and not from corrosion of the outside surface.] Further microscopic examination was performed to resolve these high wall losses and determine the actual corrosion from the outside coal-ash environment.

Microscopic Examination and EDX Analysis

Short sections from the 45-, 135-, and 270-degree locations of the samples were prepared for microscopic examination. [Note: After the evaluation it was noted that the samples from the upper probe (16,000 hours) contained the worst internal attack. Therefore, the discussion given in this report is from the upper probe.] Both probes were evaluated and detailed photomicrographs, SEM/EDX analysis, and interpretative discussions will be presented in the final report. A summary of the examination follows.

RA85H — The samples from both probes were very similar in terms of their intergranular penetration and general internal attack on the outside surface to a depth of approximately 1.5 to 2.0 mils. The worst attack was noted at the 135-degree location of sample 11, which operated at a higher temperature than sample 1. Along the surface the sample exhibited a two-part scale which consisted of a lighter scale on top of a darker scale. The lighter layer was mainly an iron-oxide scale with trace amounts of aluminum, silicon, calcium, and chromium. The darker layer was more of a chromium-rich oxide with nickel present and trace amounts of iron, aluminum, and silicon. Subsurface, the sample exhibited needle-like phases which consisted mainly of aluminum and iron with trace amounts of oxygen, silicon, chromium, and nickel. The gray phase noted at the sites of intergranular penetration were comprised of chromium, aluminum, and oxygen with small amounts of silicon, molybdenum, sulfur, titanium, vanadium, iron, and nickel. Also, the alloy displayed a very light gray phase in the form of a sphere, which was thought to be a penetrating sulfide. However, the EDX analysis revealed it was most likely a chromium carbide with minute amounts of silicon, sulfur, vanadium, iron, and nickel. In addition, the ID of samples 1 and 11 was examined and found to have suffered intergranular penetration to depths of 2.8 and 3.3 mils (upper probe) and 2.3 and 3.0 mils (lower probe), respectively.

347 — Both sets of samples contained a layer of scale, which was basically chromium oxide, on top of the corroded areas. The scale also displayed trace amounts of silicon, niobium, sulfur, calcium, iron and nickel. The gray nonmetallic phase which penetrated the subsurface of the material was found to be relatively the same

---

*Sample numbers 1 through 10 are on the hotter end of the probe, while 11 through 20 are on the colder end.

material as the scale layer. Sulfide penetration to a depth of approximately 3.0 mils was also evident in each of the samples. The sulfides contained iron, nickel, manganese, chromium, and oxygen. In addition, the samples of the upper probe suffered 2.3 and 4.0 mils of sulfur penetration along the ID surface.

NF 709 — All of the samples exhibited a thin scale layer along the outside surfaces. The scale was comprised of light and dark gray layers which gave the scale a striated appearance. The dark gray layers were chromium oxide with trace amounts of aluminum, silicon, sulfur, iron, and nickel. The light gray layers were comprised mainly of iron oxide and also contained traces of aluminum, sulfur, chromium, and nickel. The subsurface of the alloy displayed various nonmetallic phases. The amorphously shaped ones consisted of chromium, oxygen, iron, nickel, aluminum, silicon, and sulfur. The spherically shaped ones were revealed as sulfides which contained oxygen, chromium, manganese, iron, and nickel.

RA253MA — The RA253MA sample that was in the hotter section revealed a more roughened and irregular surface than its cooler counterpart. Both exhibited a two-layered scale along their outside surfaces; however, the hotter sample had the thicker layers. Beneath the scale the sample displayed sulfide penetration to a depth of approximately 4.5 mils. The outer layer of scale was basically an iron oxide with notable additions of aluminum, silicon, sulfur, calcium, chromium, and nickel. The inner layer was noted as being a chromium oxide with small amounts of silicon, sulfur, iron, and nickel present. The sulfide islands contained iron, nickel, chromium, manganese, and oxygen.

HR3C — The sample from the cooler section of the probe displayed a thin scale layer along its surface and a few localized areas of attack with subjacent internal oxidation and heavy penetration. The scale had remnant fly-ash particles in it but was still recognizable as a chromium oxide with trace amounts of sulfur, silicon, manganese, iron, and nickel. A white metallic phase was noted inside the scale. It was comprised mainly of sulfur, oxygen, iron, and nickel with small amounts of chromium and manganese. The sulfide islands noted subsurface of the scale were comprised of iron, chromium, nickel, manganese, and oxygen. The subsurface oxidation was a basic chromium oxide with notable additions of aluminum, silicon, sulfur, iron, nickel, and manganese. The depth of penetration was approximately 4 mils.

671 — Both samples from both probes displayed a broken, irregular scale along their outside surfaces. In addition, the samples exhibited some shallow pitting and localized areas of subsurface attack. The scale along the outside surface had two distinct layers—a light gray and dark gray one. The light gray was a chromium oxide with some small quantities of sulfur, iron, and nickel in it. The dark gray layer was an iron oxide with traces of aluminum, silicon, chromium, and nickel. The areas of localized attack had two distinguishable phases within their boundaries. One was a chromium-oxide phase with additional components such as aluminum, titanium, iron, and nickel also being observed. The other phase resembled a sulfide island; however, it was not a sulfur phase. Rather, it was a titanium-oxide phase with trace amounts of iron, nickel, and chromium. These internal corrodents penetrated to a depth of approximately 4 mils. In addition, both samples on both probes exhibited a scale along their inside surfaces (which consisted of LSS stainless steel material). The hotter sample (sample 16)

in the upper probe contained a 1.8-mil-thick scale while the cooler sample (sample 6) exhibited a 3-mil scale. In the lower probe, the hotter sample (sample 16) contained a 5.8-mil scale and the cooler sample (sample 6) had a 4.2-mil-thick scale.

690 — Some areas of scale exfoliaton were observed in each sample. Similar to the 671 samples, all of the 690 samples displayed a very thin, chromium-rich oxide layer on the outside surface. Internal oxidation and sulfidation were also evident in all of the samples; however, the hotter samples exhibited a deeper penetration (approximately 6 mils compared to 2 to 3 mils in the cooler sections). The inside surface (which also consisted of LSS stainless steel material) contained a 2.2-mil-thick scale in the hotter section (sample 17) and a 3.3-mil-thick scale in the cooler section (sample 7). The samples in the lower probe exhibited the same inside surface scale formation; sample 17 (hotter) had a 2-mil-thick scale, and sample 7 (cooler) had a 1-mil-thick scale.

Fe_3Al — Scale exfoliation was also observed at the ID surface. The outside surface of the samples exhibited a dark gray scale with intermittent layers of a lighter gray scale. The lighter gray scale was revealed to be chromium-rich oxide which had a substantial amount of iron mixed in as well. There were also traces of calcium, potassium, silicon, and aluminum found in the light gray scale. The dark gray scale was an aluminum-rich oxide with small amounts of chromium, iron, and sulfur. Beneath the scale layer, the surface of the metal was roughened and irregular with some definite evidence of shallow pitting. A needle-like phase was noted subsurface of the material throughout the entire thickness of all of the samples. The phases were high in iron, niobium, oxygen, and aluminum, with a small amount of chromium.

310 — The 310 Ta modified alloy sample in both probes contained a thin, chromium-rich scale with embedded fly-ash particles. Beneath the scale, the material suffered from internal oxidation and sulfidation which was more pronounced on the cooler samples. The depth of penetration for the upper probe was approximately 1.5 to 2 mils for the cooler sample (sample 9) and 2.5 mils for the hotter sample (sample 19). In the lower probe, the numbers were almost the same— 2 mils for the cooler (sample 9) and 2.2 mils for the hotter (sample 19).

800H — All of the 800H samples exhibited a two-layer scale/deposit along the outside surface with some minor internal oxidation and sulfidation. The depth of the internal penetration was noted as being deeper in the hotter sections of the upper and lower probes (sample 20: upper - 5.5 mils; lower - 5.3 mils). The cooler samples displayed penetration depths of 2 mils (upper) and 3 mils (lower). The outer layer was comprised of embedded fly-ash particles. The inner layer was predominantly chromium oxide. The sulfides contained manganese, chromium, iron, and nickel.

Wastage Determination

Wastage is considered the sum total of wall loss and metal rendered ineffective because of internal penetration of corrosive species (e.g., oxides, sulfides). Since only the wastage from the outside surface is of concern, wall loss from oxidation of the inside surface must be discounted. On this basis, the wastage of the specimens determined from the macroscopic and microscopic examinations is given in Figure 1.

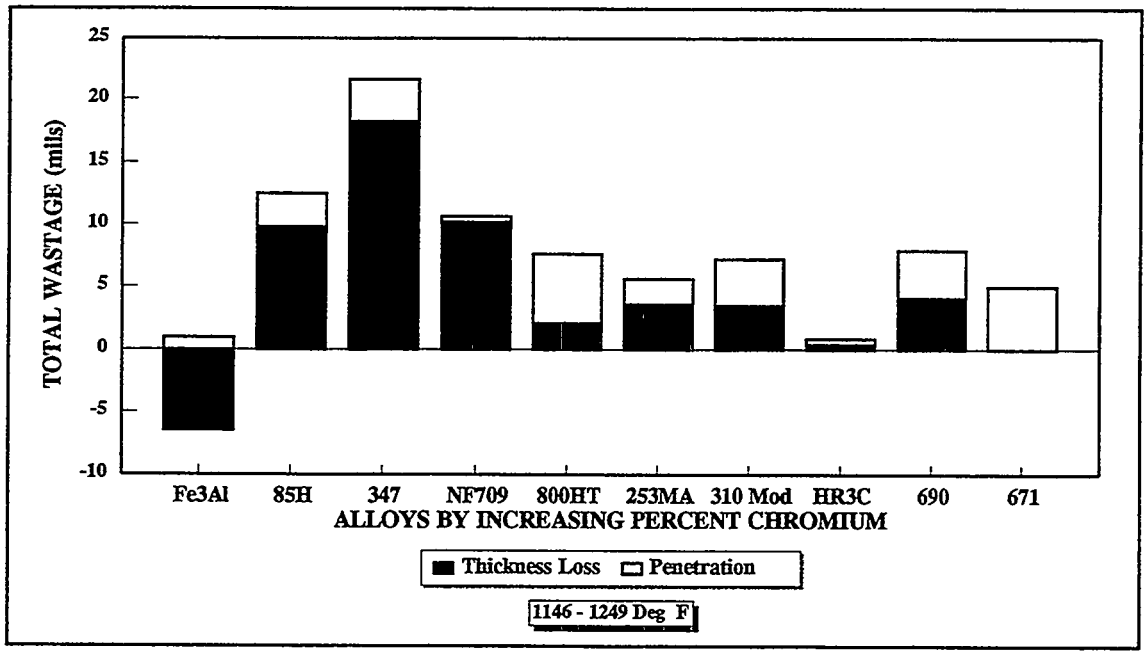

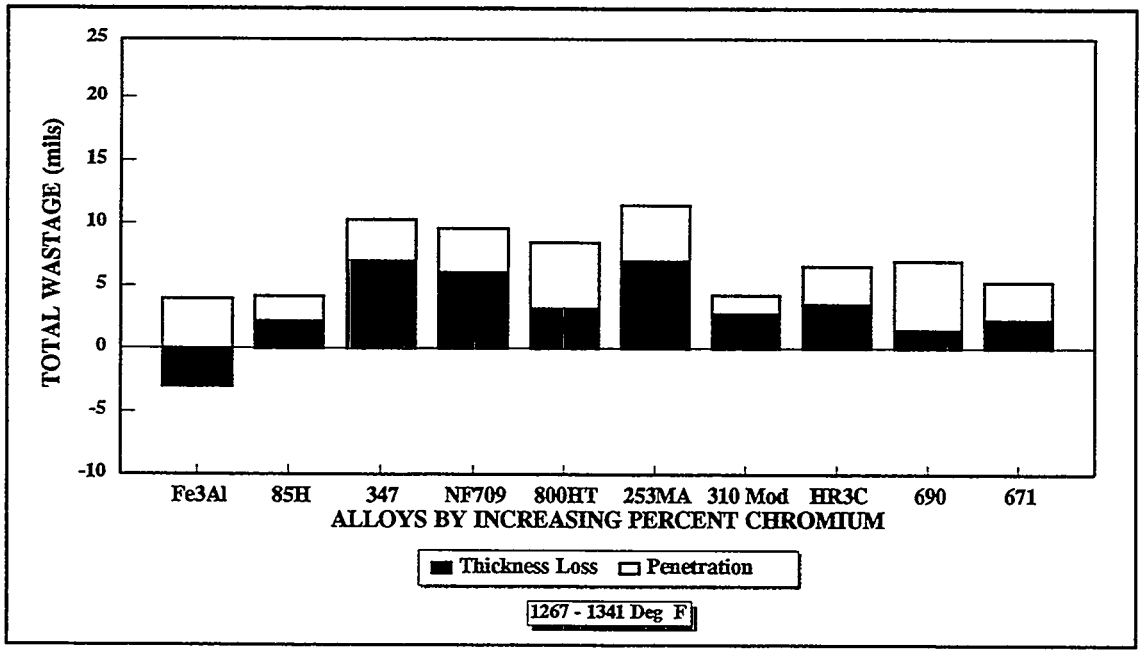

Figure 1

The upper graph lists the total wastage, including wall loss and penetration, for the samples on the 16,000-hour probe that were exposed to 1146-1249 deg F. The lower graph is for the same probe where the samples were exposed at 1267-1341 deg F.

The negative thickness losses in Figure 1 are caused by a swelling which occurred in the Fe_3Al specimens. This may be due to a phase transformation in that alloy, and further testing will have to be performed. The beneficial effect of Al and Si for the same chromium level can be observed when comparing RA85H to 347. Also, as chromium levels in the different alloys increase, there is a decrease in the corrosion rate. This is especially pronounced in the 1156 to 1249°F temperature range. Some alloys, notably RA85H, 347, and 310 Ta modified have higher corrosion rates at the lower temperature. Alloys HR3C and 253MA have a higher corrosion rate at the higher temperature, and the remaining alloys—NF 709, 800HT, 690, and 671—did not show a temperature relationship with total wastage.

These are the preliminary findings; more interpretative analysis is being performed.

CONCLUSIONS

The air-cooled, retractable corrosion probes worked successfully and provided 16,000-hour exposures of each of the nine alloys to two different temperatures.

The Fe3Al + 5Cr samples had a volume increase which is being further evaluated. The total wastage of the Fe3Al + 5Cr was 2 to 10 times lower than 347 stainless steel. The HR3C and 310 Ta modified alloy had total wastage values 2 to 3 times lower than 347 stainless steel. The 690 and the 671 samples had about the same total wastage, and the values were the same or slightly lower, respectively, than the HR3C and 310 Ta modified samples. More detailed analysis and interpretative analysis is being performed for the final report.

REFERENCES

1. W. Nelson and C. Cain, Jr., "Corrosion of Superheaters and Reheaters of Pulverized-Coal-Fired Boilers," *Transactions of the ASME, Journal of Engineering for Power,* July 1960, pp. 194-204.

2. W. T. Reid, "Formation of Alkali Iron Trisulphates and Other Compounds Causing Corrosion in Boilers and Gas Turbines," Project Review July 1, 1966-June 30, 1968, prepared by Battelle Memorial Institute, Columbus, OH, June 1968.

3. W. T. Reid, *External Corrosion and Deposits: Boilers and Gas Turbines,* American Elsevier Publishing Company, New York, 1974.

4. G. J. Hills, "Corrosion of Metals by Molten Salts," *Proceedings of the Marchwood Conference: Mechanism of Corrosion by Fuel Impurities,* Johnson and Littler, eds., Butterworths, London, 1963.

5. J. L. Blough, G. J. Stanko, M. Krawchuk, W. Wolowodiuk, and W. Bakker, "In Situ Coal Ash Corrosion Testing for 2 Years at Three Utilities," International EPRI Conference on Improved Technology for Fossil Power Plants New and Retrofit Applications, Washington, DC, March 1-3, 1993.

6. I. M. Rehn, "Fireside Corrosion of Superheater and Reheater Tubes," Palo Alto, CA: Electric Power Research Institute, 1980. CS-1653.

7. I. M. Rehn, "Fireside Corrosion of Superheater Alloys for Advanced Cycle Steam Plants," Palo Alto, CA: Electric Power Research Institute, 1987. EPRI 5195.

8. S. Van Weele and J. L. Blough, "Literature Search Update—Fireside Corrosion Testing of Candidate Superheater Tube Alloys, Coatings, and Claddings," Livingston, NJ: Foster Wheeler Development Corporation, September 1990. FWC/FWDC/TR-90-11.

9. W. Wolowodiuk, S. Kihara, and K. Nakagawa, "Laboratory Coal Ash Corrosion Tests," Palo Alto, CA: Electric Power Research Institute, July 1989. GS-6449.

10. S. Van Weele and J. L. Blough, "Fireside Corrosion Testing of Candidate Superheater, Tube Alloys, Coatings, and Claddings," Livingston, NJ: Foster Wheeler Development Corporation, August 1991. ORNL/SUB/89-SA187/02.

11. S. Kihara, K. Nakagawa, A. Ohtomo, H. Aoki, and S. Ando, "Simulating Test Results for Fireside Corrosion of Superheater & Reheater Tubes Operating at Advanced Steam Conditions in Coal-Fired Boilers, *High Temperature Corrosion in Energy Systems,* TMS/AIME, M. F. Rothman, ed., 1984, pp. 361-376.

12. W. Wolowodiuk, et al., "Coal-Ash Corrosion Investigations," *Proceedings of the First International Conference on Improved Coal-Fired Power Plants.* Palo Alto, CA: Electric Power Research Institute, November 1986.

13. J. L. Blough, M. T. Krawchuk, G. J. Stanko, and W. Wolowodiuk, "Superheater Corrosion Field Test Results," Palo Alto, CA: Electric Power Research Institute, November 1993. TR-103438.

14. J. L. Blough and W. T. Bakker, "Measurement of Superheater Corrosion Caused by Molten Alkali Sulfates," First International Conference on Heat-Resistant Materials, to be presented at the ASM International, Lake Geneva, WI, September 22-26, 1991.

15. T. Hammond, W. Wolowodiuk, J. L. Blough, J. Brooks, "Replacement of Reheater at TVA's Gallatin Station Unit 2," presented at the Third International Conference on Improved Coal-Fired Power Plants (ICPP), San Francisco, April 1991.

16. R. W. Borio and R. P. Hensel, "Coal-Ash Composition as Related to High-Temperature Fireside Corrosion and Sulfur-Oxides Emission Control," *Transactions of the ASME, Journal of Engineering for Power,* Vol. 94, 1972, pp. 142-148.

17. J. L. Blough, "Fireside Corrosion Testing of Candidate Superheater, Tube Alloys, Coatings, and Claddings," Livingston, NJ: Foster Wheeler Development Corporation, August 1996. ORNL/SUB/93-SM401/01.

PROCESSING AND PROPERTIES OF MOLYBDENUM SILICIDE INTERMETALLICS CONTAINING BORON

J. H. Schneibel, C. T. Liu, L. Heatherly, J. L. Wright, and C. A. Carmichael

Oak Ridge National Laboratory
P. O. Box 2008
Oak Ridge, Tennessee, U. S. A.

ABSTRACT

Molybdenum-silicon-boron intermetallics with the composition Mo-10.5 Si-1.1 B, wt% (Mo-26.7 Si-7.3 B, at. %) were fabricated by several processing techniques. Powder processing (PM) resulted in macrocrack-free material containing no or only few microcracks. The PM materials contained quasi-equilibrium pores and large concentrations of oxygen. Average room temperature flexure strengths of 270 MPa were obtained. At 1200°C in air, flexure strengths as high as 600 MPa were observed. These high values are attributed to crack healing and incipient plasticity. Ingot metallurgy (IM) materials contained much less oxygen than their PM counterparts. Depending on the cooling rate during solidification, they developed either mostly macrocracks or mostly microcracks. Due to the high flaw densities, the room temperature flexure strengths were only of the order of 100 MPa. However, the flexure strengths at 1200°C were up to 3 times higher than those at room temperature. Again, this is attributed to crack healing and incipient plasticity. The IM materials will require secondary processing to develop their full potential. A preliminary examination of secondary processing routes included isothermal forging and hot extrusion.

INTRODUCTION

The objective of this task is to develop new-generation corrosion-resistant Mo-Si alloys for use as hot components in advanced fossil energy combustion and conversion systems. The successful development of Mo-Si alloys is expected to improve the thermal efficiency and performance of fossil energy conversion systems through an increased operating

temperature, and to increase the service life of hot components exposed to corrosive environments at temperatures as high as 1600°C. While $MoSi_2$ is highly oxidation resistant at elevated temperatures, it is extremely brittle at ambient temperatures. Molybdenum compounds with lower Si contents, such as Mo_5Si_3, which are potentially less brittle, do however, not have the required oxidation resistance. As will be seen, boron additions are the answer to the oxidation problem.

As early as 1957, Nowotny et al.[1] pointed out that boron-containing silicides possess high oxidation resistance due to the formation of borosilicate glasses. Based on Nowotny et al's work, boron-containing molybdenum silicides based on Mo_5Si_3 were recently developed at Ames Laboratory.[2-4] These silicides consist of approximately 50 vol.% Mo_5Si_3 (T1), 25 vol.% Mo_5SiB_2 (T2), and 25 vol.% of Mo_3Si. They provide an exciting alternative to $MoSi_2$ for several reasons. First, they possess an oxidation resistance comparable to that of $MoSi_2$, and do not show catastrophic oxidization ("pest reaction") at intermediate temperatures such as 800°C.[4] Second, these three-phase materials may possess a higher fracture resistance than other high-temperature materials such as $MoSi_2$. Third, their creep strength is superior to that of $MoSi_2$.

At present, the mechanical properties of the new Mo-Si-B alloys have not been fully explored. One reason for this is simply the unavailability of sufficiently large test pieces. Due to the high processing temperatures and the high reactivity of Si, processing of Mo-Si-B alloys with good quality is a challenging task. Significant developmental work is, therefore, needed to produce sound Mo-Si-B material with controlled microstructures. At the same time the size of the material must be sufficient (e.g., 50 mm) to be able to characterize the mechanical properties. An interaction between processing, microstructural characterization, and mechanical property measurements is required in order to improve and optimize this new class of materials.

RESULTS AND DISCUSSION

Processing via powder metallurgy

A previous annual report for this program[5] focused on powder metallurgical (PM) processing. Some additional microstructural, mechanical property, and compositional work is reported here. Based on the composition Mo-10.5 Si-1.1 B (wt%), four PM alloys (see also Table I) were produced by hot-pressing. In several cases, carbon was

added to reduce the oxygen content. For the same reason, additions of Zr were made. The difference between the two approaches is that Zr removes oxygen in the form of internal oxides, while carbon additions remove oxygen in the form of gaseous CO/CO_2. Zirconium additions resulted in internal cracking, due to the formation of ZrO_2 particles and the associated thermal expansion mismatch. The Zr-containing alloys were therefore not further investigated.

The oxygen contents of several PM as well as cast Mo-Si-B materials are summarized in Table I. Several points are worth noting. First, the alloy MSB1, which was fabricated from $MoSi_2$ powder and addition of elemental powders, has by far the highest oxygen content. Second, as the carbon content is increased from 0.6 wt% (MSB2) to 1.0 wt% (MSB5), the oxygen content tends to decrease. This indicates that the carbon was indeed effective in deoxidizing the alloys. Third, as expected, the cast materials (MSB418 and MSB424) have much lower oxygen contents than the PM materials.

Table I. Compositions and oxygen contents of Mo-Si-B alloys

Sample ID	Processing*	Composition, wt%	Oxygen, wppm*
MSB1	PM/HP	Mo-10.5 Si-1.1 B-0.2 C	7482
MSB2, analysis #1	PM/HP	Mo-10.41 Si-1.09 B-0.60 C-0.20 Zr	3195
MSB2, analysis #2	PM/HP	"	2275
MSB3	PM/HP	Mo-10.4 Si-1.1B-1.0C	
MSB5	PM/HP	Mo-10.4 Si-1.1B-1.0C	
MSB5	PM/HP	Mo-10.4 Si-1.1 B-1.0 C	1938
MSB418 (center region)	IM(Cu mold)	Mo-10.5 Si-1.1 B	486
MSB418 (near surface)	IM (Cu mold)	"	222
MSB424	IM (C mold)	"	217
MSB425	IM (sand mold)	"	
MSB465	IM (Al_2O_3/SiO_2 mold)	"	

* processing by powder metallurgy (PM) and hot pressing (HP), or by ingot metallurgy (IM).

**The oxygen contents are courtesy M. J. Kramer, Ames Laboratory, Ames, Iowa

Figure 1 illustrates the microstructure of a polished and etched specimen of alloy MSB1, which contained 0.2 wt% C as deoxidizer. The scanning electron microscope (SEM) image in Fig. 1 shows no microcracks, although a more detailed examination of the specimen from which this micrograph was obtained, revealed occasional microcracks. Numerous pores are seen at the grain and interphase boundaries. Their quasi-equilibrium

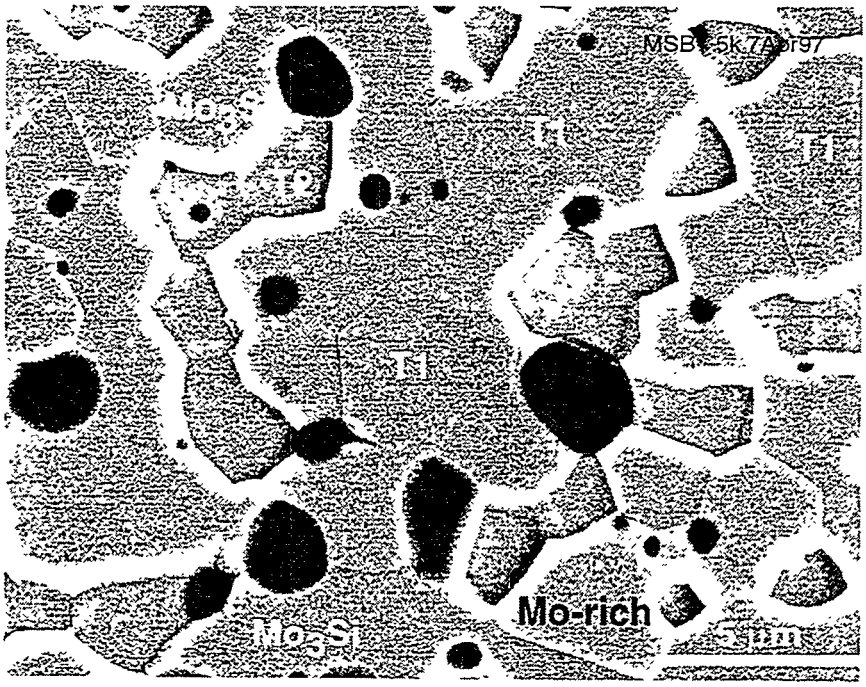

Fig. 1. SEM micrograph of alloy MSB1 (Mo-10.5 Si-1.1 B-0.2 C, wt%) after polishing and etching (Murakami's etch). Pores appear in black. The T2 phase (Mo_5SiB_2) is preferentially etched. In addition to Mo_3Si and Mo_5Si_3 (T1), a Mo-rich phase is found, which is either unreacted Mo or a boride of Mo.

shape suggests that they may have been stabilized by trapped CO/CO_2. The different phases were identified via energy dispersive spectroscopy (EDS) in the SEM. Since B was difficult to detect, identification was performed on the basis of the Si to Mo ratio. The T2 phase (Mo_5SiB_2) etched readily and was therefore easily recognized. Occasionally Mo-rich particles were found. These are either elemental Mo or borides of Mo. The fact that the three-phase Mo_3Si-T1-T2 equilibrium expected from the nominal composition[1] has not been reached is consistent with recent results by Perepezko et al.[6] These authors found that annealing of similar alloys for 150 h at 1600°C did not establish complete phase equilibrium. Since the hot-pressing in this work was carried out at 1600°C, it is not surprising that full equilibrium was not reached.

Processing via ingot metallurgy

Alloys with the composition Mo-10.5 Si-1.1 B (wt%) were drop-cast into molds made from materials with different thermal conductivities in order to examine the effect of the cooling rate on the microstructures that developed during solidification and cool-down. Casting into a 25 mm diam. Cu mold produced ingots which appeared to be uncracked as

judged by visual examination of their outside. However, sectioning and polishing of these ingots always revealed macroscopic cracking. The microstructure of a cast and annealed specimen is shown in Fig. 2. Voids were not detected, but microcracks were occasionally observed. As shown in Table I, the IM alloys contained much less oxygen than the PM alloys.

Casting Mo-10.5 Si-1.1 B into a 25 mm diam. SiO_2 (sand) mold resulted in much lower cooling rates and eliminated macroscopic cracking. An approximately 1 mm thick reaction zone was observed on the outside of the ingot. A typical microstructure is illustrated in Fig. 3. As compared to Fig. 2, more microcracking is seen. Although a quantitative analysis has not been carried out, it appears that the lower cooling rate enhances microcracking. Since Mo_5Si_3 exhibits anisotropic thermal expansion, slower cooling and the associated larger grain/phase sizes are likely to enhance microcracking.

Casting Mo-10.5 Si-1.1 B into a 25 mm diam. porous Al_2O_3/SiO_2 mold resulted in the slowest cooling rate. Solidification occurred so slowly, that the melt reacted extensively with the mold. After cool-down, the casting had a diameter of approximately 50 mm, instead of the initial mold diameter of 25 mm. As verified by qualitative EDS analysis, this alloy picked up significant amounts of oxygen. No macrocracks were observed, but many microcracks. Figure 4 illustrates the microcracks found in this material. Interestingly, the microcracks stopped often in the T2 phase. The microstructure is much coarser than that of the other alloys (compare for example Figs. 4 and 2). Therefore, while macrocracking was alleviated, microcracking was enhanced.

Isothermal forging

An attempt was made to isothermally forge a cylindrical section of an alloy cast into a sand mold (MSB425). This experiment was carried out in a hot-pressing unit. An initial pressure of 35 MPa was applied. Consistent with the excellent high temperature strength of this material no deformation occurred at temperatures up to 1800°C. At 1850°C, the specimen deformed by approximately 50% in 15 minutes . The external appearance of the deformed specimen suggested that the material was partially liquid during deformation.

Microstructural analysis showed that some voids and cracks had formed during the processing. Since the material was partially liquid, this is not surprising.

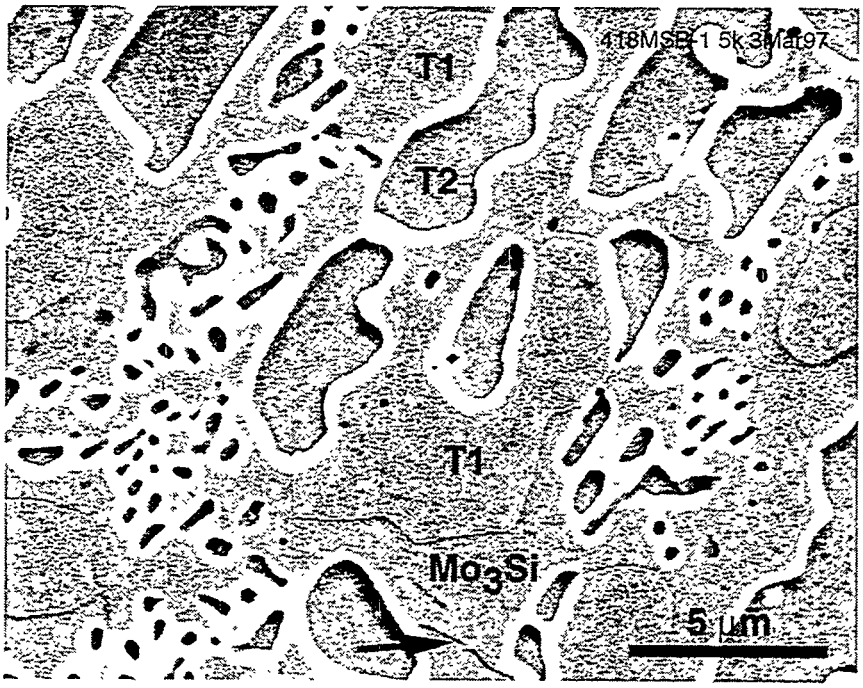

Fig. 2. SEM micrograph of polished and etched section of Mo-10.5 Si-1.1 B cast into a 25 mm diam. Cu mold and annealed for 24 h at 1400°C in vacuum (MSB418). The three phases expected according to the phase diagram[1] are all seen. The T2 phase is preferentially attacked by Murakami's etch. The absence of significant porosity is noted. A microcrack is indicated by an arrow.

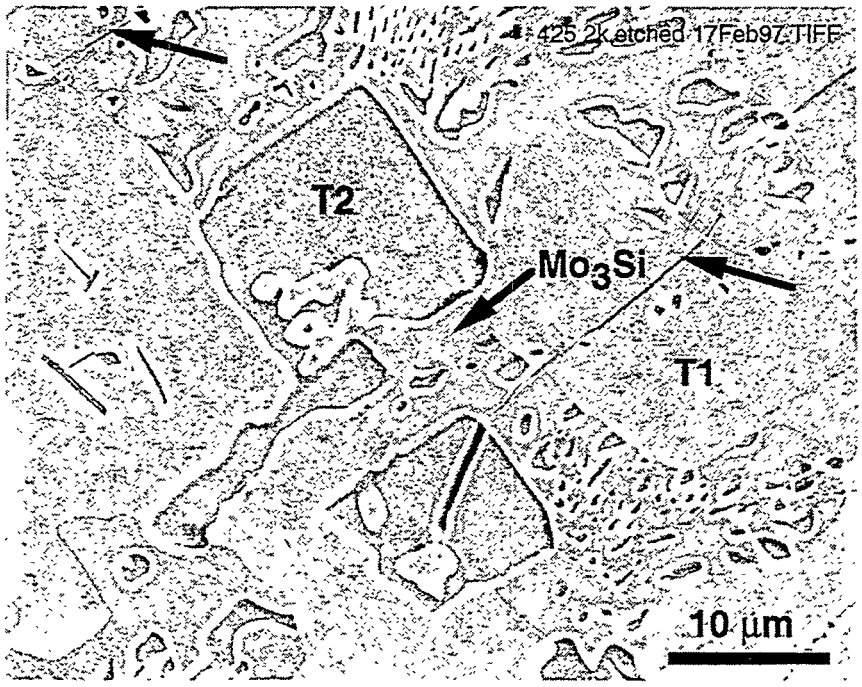

Fig. 3. SEM micrograph of polished and etched section of Mo-10.5 Si-1.1 B cast into a 25 mm diam. sand mold (MSB425). Several microcracks are indicated by arrows.

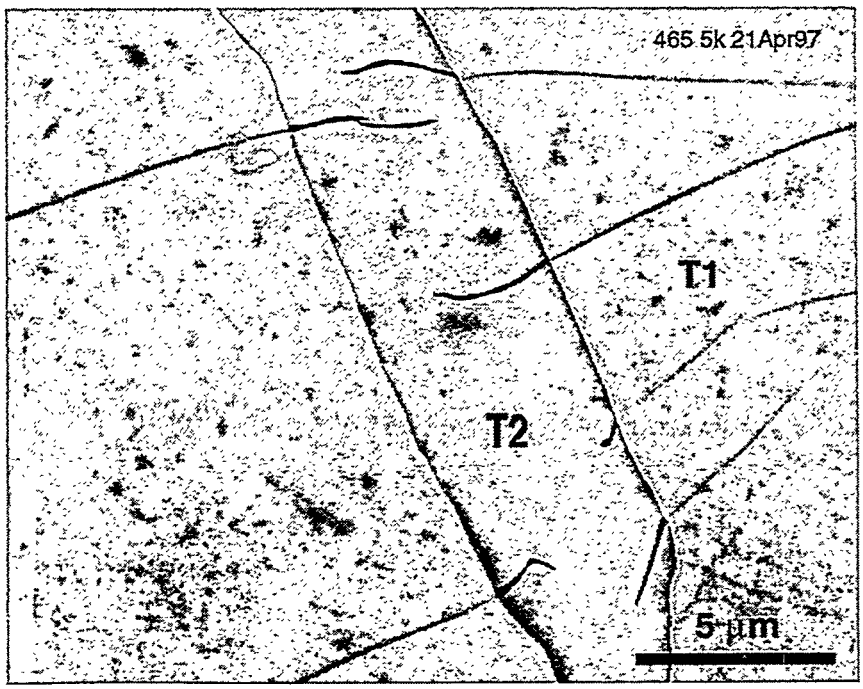

Fig. 4. SEM micrograph of polished and etched section of Mo-10.5 Si-1.1 B cast into a 25 mm diam. Al_2O_3/SiO_2 mold (MSB465).

Extrusion

A casting with the composition Mo-10.5 Si-1.1 B (MSB418) was encapsulated in an evacuated Mo can and extruded at 1800°C. The extrusion exhibited severe cracking and porosity and only small pieces were available for metallographic examination. Figure 5 shows an SEM of the extruded materials. According to EDS analysis, the microstructure consisted of particles of Mo_3Si (dark phase) in a multiphase matrix. In agreement with the EDS finding, x-ray analysis indicated Mo_3Si to be the majority phase. The x-ray analysis revealed also Mo and the T2 phase. The multiphase matrix found between the Mo_3Si particles is depicted in Fig. 6. Due to the small scale, a reliable EDS analysis was not possible. The x-ray analysis suggested that the matrix consists of Mo, Mo_3Si, and T2. Since the nominal composition of the extruded material should have resulted in a 3-phase mixture of Mo_3Si, T1, and T2, it appears that the Mo content of the extruded material increased by a reaction with the Mo can. Since liquid phase formation was observed during isothermal forging at 1850°C, and since the presence of Mo in the extrusion experiment may have reduced the liquidus temperature, liquid phase formation is plausible.

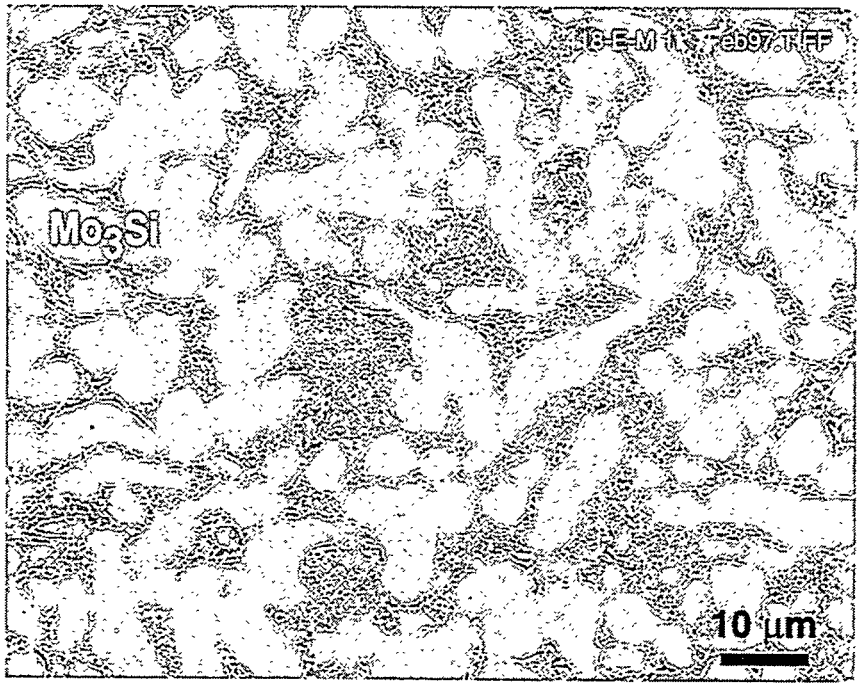

Fig. 5. SEM micrograph of a polished/etched section of extruded Mo-Si-B (MSB418-E).

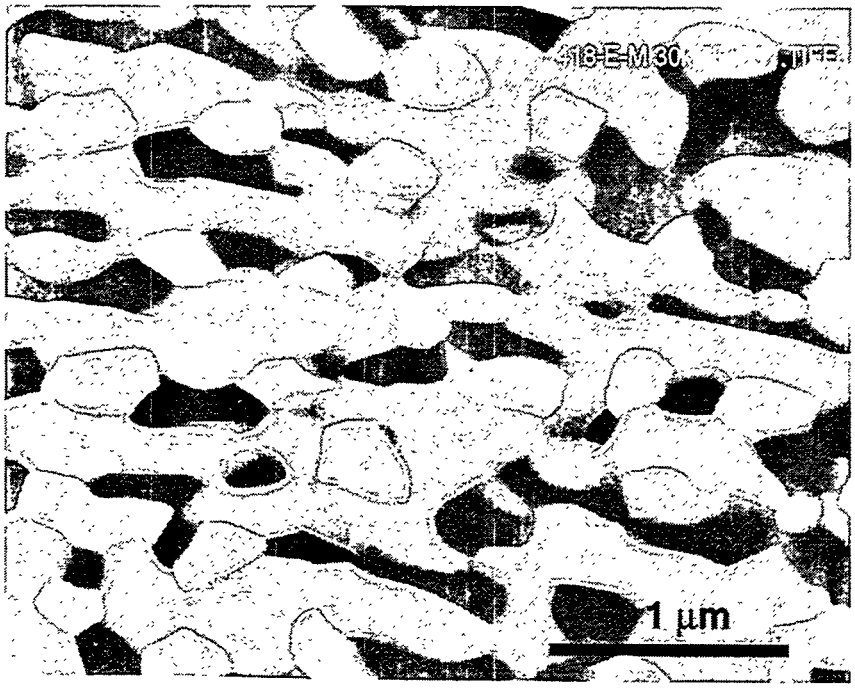

Fig. 6. High magnification SEM micrograph of matrix region of polished and etched section of extruded Mo-Si-B (MSB418-E).

It is, however, encouraging that the extrusion resulted locally in a very fine structure.

Mechanical properties

In a previous report[5] the room temperature tensile strength of the PM alloy MSB1 was determined to be 186 MPa. Since the silicides investigated in this work are flaw-sensitive, it was decided to carry out a larger number of flexure tests in order to obtain statistical information. The results are represented in the Weibull plot in Fig. 7. They indicate that flexure strengths of up to 300 MPa may be obtained. Since this particular material contained porosity (see Fig. 1) as well as a substantial concentration of oxygen (Table I), significantly better properties are expected for optimized processing. Table II shows that the flexure strength is substantially higher at 1200°C, where it reaches values as high as

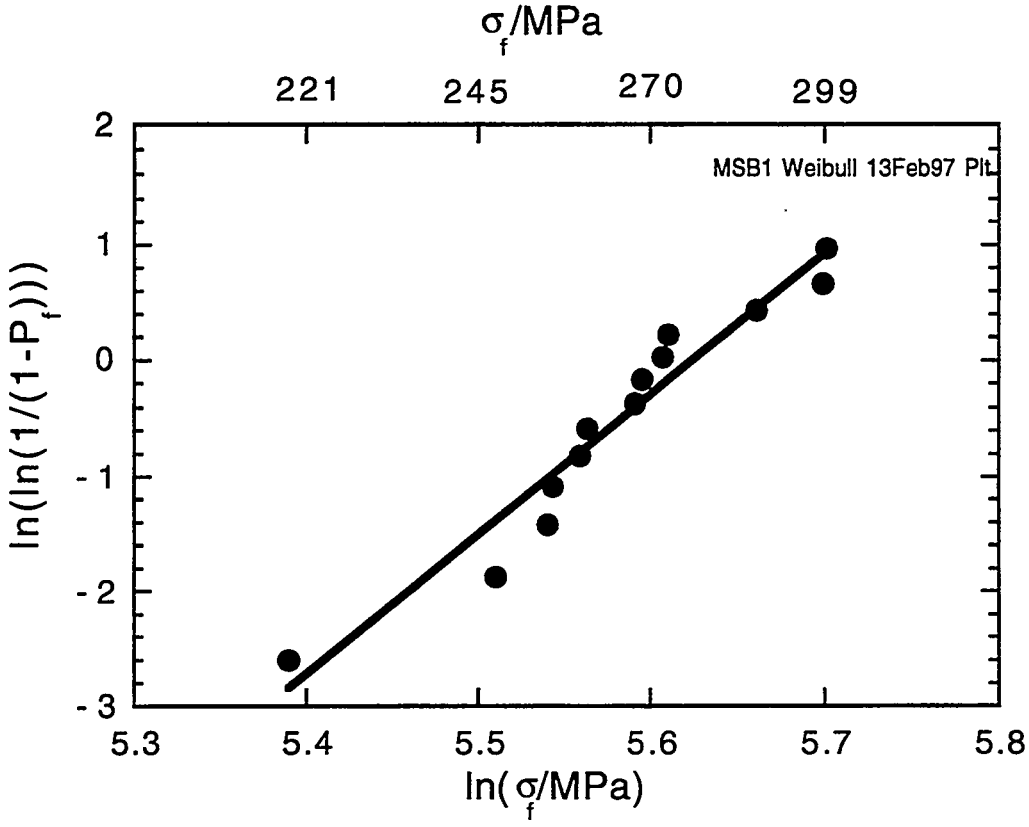

Fig. 7. Weibull Plot of the 3-point flexure strength of MBS1 (Mo-10.5 Si-1.1 B-0.2 C, wt%). P_f is the fracture probability, and σ_f the maximum outer fiber stress.

Table II. Three-point flexure strengths of Mo-10.5 Si-1.1 B (wt%)

Specimen Number	Processing*	Specimen Condition	Test Temperature, ℃	Fracture Strength, MPa
MSB1	PM	as-pressed, average of 13 specimens	20	270
"	PM	as-pressed	1200	460
"	PM	as-pressed	1200	604
MSB425	IM	as-cast	20	119
"	IM	as-cast	20	105
"	IM	as-cast	20	114
"	IM	isothermal forging at 1850°C	20	95
"	IM	isothermal forging at 1850°C	20	110
"	IM	as-cast	1200	221
"	IM	as-cast	1200	283

*PM:powder metallurgy, IM: ingot metallurgy

604 MPa. The high strength may be due to crack healing, borosilicate glass formation at crack tips, or incipient plasticity. The two specimens tested at 1200°C showed quite different strengths indicating that further processing improvements will be needed.

Whereas the PM processed silicides contain no or few microcracks, the cast silicides do. The cast materials are therefore expected to have lower room temperature strengths than the powder metallurgical ones. Table II shows this to be the case. Consistent with the observation of microcracks, isothermal forging at 1850°C (which did cause incipient melting) did not improve the room temperature strength. At elevated temperatures, the microcracks may not be as detrimental to the strength than at room temperature. This could be caused by crack healing, crack blunting, as well as borosilicate glass formation at crack tips. Consistent with this, the 1200°C flexure strengths determined in air are 2 to 3 times higher than those at room temperature, as demonstrated by the data in Table II. This result points out the continuing importance of optimizing the processing of these materials in order to achieve satisfactory mechanical properties. In the case of the IM materials, secondary processing is definitely required in order to minimize the size and number density of microcracks. Efforts are underway to improve the secondary processing.

SUMMARY AND CONCLUSIONS

Molybdenum-silicon-boron intermetallics with the composition Mo-10.5 Si-1.1 B (wt%) were fabricated by several processing techniques. Powder processing resulted in macrocrack-free material containing no or few microcracks. PM materials exhibited reasonably high room temperature strength and excellent strength at 1200°C in air. However, they contained quasi-equilibrium pores, and large concentrations of oxygen. Ingot metallurgy (IM) materials showed much lower oxygen concentrations. Depending on the cooling rate during solidification, they developed either mostly macrocracks or mostly microcracks. Due to the microcracks, the room temperature flexure strengths were low. However, the flexure strengths at 1200°C were up to 3 times higher than those at room temperature. This is attributed to processes such as crack healing, borosilicate glass formation, and incipient plasticity. The IM materials require secondary processing to develop their full potential. Preliminary examinations of secondary processing include isothermal forging and hot extrusion, and further work is in progress to improve the secondary processing.

ACKNOWLEDGMENTS

The authors would like to thank M. J. Kramer, Ames Laboratory, for kindly providing the oxygen concentration data. Thanks are due to J. A. Horton and C. G. McKamey for reviewing this manuscript. This research was sponsored by the Fossil Energy Advanced Research and Technology Development (AR&TD) Materials Program, U.S. Department of Energy, under contract DE-AC05-96OR22464 with Lockheed Martin Energy Research Corporation.

REFERENCES

1. H. Nowotny, E. Kimakopoulou, and H. Kudielka, "Untersuchungen in den Dreistoffsystemen: Molybdän-Silizium-Bor, Wolfram-Silizium-Bor und in dem System: VSi_2-$TaSi_2$," Mh. Chem. 88 (1957) 180
2. A. J. Thom, M. K. Meyer, Y. Kim, and M. Akinc, "Evaluation of $A_5Si_3Z_x$ Intermetallics for Use as High Temperature Structural Materials," in "Processing and Fabrication of Advanced Materials III, V. A. Ravi et al., eds., TMS, 1994, p. 413.
3. M. K. Meyer, M. J. Kramer, and M. Akinca [sic], "Compressive Creep Behavior of Mo_5Si_3 with the Addition of Boron," Intermetallics 4 (1996) 273.
4. M. Meyer, M. Kramer, and M. Akinc, "Boron-Doped Molybdenum Silicides," Adv. Mater. 8 (1996) 85.

5. Fossil Energy Program Annual Progress Report for April 1995 through March 1996, R. R. Judkins, Program Manager, ORNL-6902, pp. 157-167.
6. J. H. Perepezko, C. A. Nuñes, S.-H. Yi, and D. J. Thoma, "Phase Stability in Processing of High Temperature Intermetallic Alloys," in press, MRS Symposium Proceedings Vol. 460, C. C. Koch et al., eds.

APPENDIX A

FINAL PROGRAM

FINAL PROGRAM
CONFERENCE ON FOSSIL ENERGY MATERIALS
Knoxville, Tennessee
May 20-22, 1997

SESSION I - Ceramic Composites and Functional Materials

Tuesday, May 20, 1997

7:00 **Registration and Continental Breakfast**

8:00 *Welcome and Introductory Remarks*, Program Managers, Department of Energy and Oak Ridge National Laboratory

8:20 *Advanced Research Programs and AR&TD Materials Program Overview*- R.R. Judkins, Fossil Energy Program Manager, Oak Ridge National Laboratory

9:00 *Development of a Scale-Up CVI System for Tubular Geometries,* T. M. Besmann, Oak Ridge National Laboratory

9:30 *Mass Transport Measurements and Modeling for Chemical Vapor Infiltration,* T. L. Starr, Georgia Institute of Technology

10:00 **BREAK**

10:20 *Development of Oxidation-Resistant Composite Materials and Interfaces,* R.A. Lowden, Oak Ridge National Laboratory

10:50 *Corrosion Protection of SiC Based Ceramics with CVD Mullite Coatings,* V. Sarin, Boston University

11:20 *Thermal Cycling Characteristics of Plasma Synthesized Mullite Films*, I. Brown, Lawrence Berkeley National Laboratory

11:50 **LUNCH**

1:15 *Influence of Water Vapor and Slag Environments on Corrosion and Mechanical Properties of Ceramic Materials*, K. Natesan, Argonne National Laboratory

1:45 *Evaluation of an All-Ceramic Tubesheet Assembly for a Hot Gas Filter*, J. L. Bitner, Mallett Technology

2:15 *Development of Nondestructive Evaluation Methods for Structural Ceramics*, W. A. Ellingson, Argonne National Laboratory

2:45 **BREAK**

3:00 *Solid State Electrolyte Systems*, L. R. Pederson, Pacific Northwest Laboratory

3:30 *Activation and Micropore Structure Determination of Carbon-Fiber Composite Molecular Sieves*, M. Jagtoyen, University of Kentucky Center for Applied Energy Research

4:00 *A Carbon Fiber Based Monolithic Adsorbent for Gas Separation*, T. D. Burchell, Oak Ridge National Laboratory

4:30 **ADJOURN**

FINAL PROGRAM
CONFERENCE ON FOSSIL ENERGY MATERIALS
Knoxville, Tennessee
May 20-22, 1997

SESSION II - Ceramics, New Alloys, and Functional Materials

Tuesday, May 20, 1997
6:30 - 8:30 p.m.

POSTER PRESENTATIONS - BUFFET RECEPTION

Mechanical Performance of Hi-Nicalon/CVI-SiC Composites with Multilayer SiC/C Interfaces, W. A. Curtin, Virginia Polytechnic Institute and State University

Heat Treatment Effects for Improved Creep-Rupture Resistance of a Fe_3Al-based Alloy, C. G. McKamey, Oak Ridge National Laboratory

Effects of Humidity and Test Frequency on Environmental Embrittlement of Fe_3Al Alloys , N. S. Stoloff, Rensselaer Polytechnic Institute

Effects of Titanium and Zirconium on Iron Aluminide Weldments, G. R. Edwards, Colorado School of Mines

Effects of 1000 °C Oxide Surfaces on Room Temperature Aqueous Corrosion and Environmental Embrittlement of Iron Aluminides, R. A. Buchanan, University of Tennessee

Coal-Based Carbon Products: Processes, Applications, and Future Challenges, C. Irwin, West Virginia University

The Influence of Processing on Microstructure and Properties of Iron Aluminides, R. N. Wright, Idaho National Engineering Laboratory

Mechanisms of Defect Complex Formation and Environmental-Assisted Fracture Behavior of Iron Aluminides, B. R. Cooper, West Virginia University

Ultrahigh Temperature Intermetallic Alloys, C. T. Liu and M. Brady, Oak Ridge National Laboratory

Study of Fatigue and Fracture Behavior of Cr_2Nb-Based Alloys:Phase Stability in Nb-Cr-Ni Ternary Systems, P. Liaw, University of Tennessee

Iron-Aluminide Filters for IGCCs and PFBCs, P. F. Tortorelli, Oak Ridge National Laboratory

Weld Overlay Cladding With Iron Aluminides, G. M. Goodwin, Oak Ridge National Laboratory

SHS Processing and Properties of Intermetallic Alloys and Composites, R. Walters, Albany Research Center

Ceramic Membranes For High Temperature Hydrogen Separation, G. Roettger, East Tennessee Technology Park

High Temperature Corrosion Behavior of Iron-Aluminide Alloys and Coatings, P. F. Tortorelli, Oak Ridge National Laboratory

Corrosion-Resistant Coating Devlopment, D. P. Stinton, Oak Ridge National Laboratory

FINAL PROGRAM
CONFERENCE ON FOSSIL ENERGY MATERIALS
Knoxville, Tennessee
May 20-22, 1997

SESSION III - WORKSHOP

Wednesday, May 21, 1997

MORNING SESSION - Materials Issues in Low-Emission Boilers

7:00	**Registration and Continental Breakfast**
8:00	**Keynote Address: Mr. L. A. Ruth** **Federal Energy Technology Center** **Pittsburgh, Pennsylvania**
8:30	N. Birks, University of Pittsburgh
9:00	LEBS/T. B. Gibbons, ABB Combustion Engineering
9:20	LEBS/P. Daniel, Babcock & Wilcox
9:40	LEBS/Riley Stoker
10:00	**BREAK**
10:20	*Update on Low-NO_x Issues*, R. B. Dooley, EPRI
10:40	*Critical Materials Issues*, C. D. Lundin, University of Tennessee
11:00	Discussion
12:00	**LUNCH**

AFTERNOON SESSION - Materials Issues in High Efficiency Coal-Fired Cycles

1:30	*Review of UTRC's HIPPS Development*, John Holowczak
2:15	*Review of Foster Wheeler's HIPPS Development*, Jeff Blough
3:00	**BREAK**
3:20	*SiC-Based Ceramics in Coal Combustion Environments*, Kristin Breder, Oak Ridge National Laboratory
3:50	*Modifications of Slags and Monolithic Refractories to Reduce Corrosion Rates,* John Hurley, University of North Dakota Energy and Environmental Research Center
4:20	**ADJOURN**

FINAL PROGRAM
CONFERENCE ON FOSSIL ENERGY MATERIALS
Knoxville, Tennessee
May 20-22, 1997

SESSION IV - New Alloys

Thursday, May 22, 1997

7:30 **Registration and Continental Breakfast**

8:00 *Welcome and Introductory Remarks*

8:10 *Development of ODS Fe_3Al Alloys,* I.G.Wright , Oak Ridge National Laboratory

8:40 *Iron Aluminide Weld Overlay Coatings for Boiler Tube Protection in Coal-fired Low NOx Boilers*, J. N. DuPont, Lehigh University

9:10 *Corrosion Performance of Iron Aluminides in Fossil Energy Environments* K. Natesan, Argonne National Laboratory

9:40 *Microstructure of Mechanical Behavior of Alumina Scales and Coatings,* K. B. Alexander, Oak Ridge National Laboratory

10:10 **BREAK**

10:30 *Microstructural and Mechanical Property Characterization of Ingot Metallurgy ODS Iron Aluminum,* V. K. Sikka, Oak Ridge National Laboratory

11:00 *Simulataneous Aluminizing and Chromizing of Steels to Form $(Fe,Cr)_3Al$ Coatings and Ge-doped Silicide Coatings of Cr-Zr Base Alloys,* R. A. Rapp, Ohio State University

11:30 *Electro-Spark Deposition Technology,* R. N. Johnson, Pacific Northwest Laboratory

12:00 **LUNCH**

1:15 *Investigation of Austenitic Alloys for Advanced Heat Recovery and Hot-Gas Cleanup Systems,* R. W. Swindeman, Oak Ridge National Laboratory

1:45 *Fireside Corrosion Testing of Candidate Superheater Tube Alloys, Coatings, and Claddings - Phase II,* J. L. Blough, Foster Wheeler Development Corporation

2:15 *Processing and Properties of Molybdenum Silicide Intermetallics with Boron,* J. H. Schneibel, Oak Ridge National Laboratory

2:45 **ADJOURN**

APPENDIX B

LIST OF ATTENDEES

ATTENDEE LIST

Fossil Energy Materials Conference
May 20-22, 1997
Knoxville, Tennessee

A
Shawn Ailey
Oak Ridge National Laboratory
P.O. Box 2008
Oak Ridge, TN 37831-6064
(423) 576-5086
FAX 423-574-4913

Kathi Alexander
Oak Ridge National Laboratory
P.O. Box 2008
Oak Ridge, TN 37831-6376
(423) 574-0631
FAX 423-574-0641

David Alman
Albany Research Center
1450 Queen Avenue SW
Albany, OR 97321
(541) 967-5885
FAX 541-967-5845

Mark J. Andrews
U.S. Department of Energy
Oak Ridge National Laboratory
P.O. Box 2008
Oak Ridge, TN 37831-6069
(423) 241-4571
FAX 423-574-6098

B
Stephen W. Banovic
Lehigh University
Energy Research Center
Whitaker Laboratory
5 E Packer Avenue
Bethlehem, PA 18015
(610) 758-4270
FAX 610-758-4244

Paul Becher
Oak Ridge National Laboratory
P.O. Box 2008
Oak Ridge, TN 37831-6068
(423) 574-5157
FAX 423-574-6098

Barbara Bennett
Oak Ridge National Laboratory
P.O. Box 2008
Oak Ridge, TN 37831-6087
(423) 574-5220

Theodore Besmann
Oak Ridge National Laboratory
P.O. Box 2008
Oak Ridge, TN 37831-6063
(423) 574-6852
FAX 423-574-4913

Neil Birks
The University of Pittsburgh
Materials Science & Engineering Dept.
848 Benedum Hall
Pittsburgh, PA 15261
(412)624-9743
FAX 412-624-8069

Jerry Bitner
Mallett Technology
100 Park Drive
Suite 204
P.O. Box 14407
Research Triangle Park, NC
FAX 412-746-7001

Jeff Blough
Foster Wheeler Development Corp.
John Blizard Research Center
12 Peach Tree Hill Road
Livingston, NJ 07039-5701
(201) 535-2355
FAX 201-535-2242

Ron Bradley
Oak Ridge National Laboratory
P.O. Box 2008
Oak Ridge, TN 37831-6161
(423) 574-6095

Mike Brady
Oak Ridge National Laboratory
P.O. Box 2008
Oak Ridge , TN 37831-6115
(423) 576-2449
FAX 423-574-5118

Kristin Breder
Oak Ridge National Laboratory
P. O. Box 2008
4515, MS 6062
Oak Ridge, TN 37831-6062
(423) 574-5089
FAX 423-574-4913

Ian Brown
University of California
Lawrence Berkeley Laboratory
One Cyclotron Road
Bldg 53
Berkeley, CA 94720
(510) 486-4174
FAX 510-486-4374

R. A. Buchanan
The University of Tennessee
Department of Materials Science and Engineering
434 Dougherty Engineering Building
Knoxville, TN 37996-2200
(423) 974-4858

Tim Burchell
Oak Ridge National Laboratory
P. O. Box 2008
4508, MS 6088
Oak Ridge, TN 37831-6088
(423) 576-8595
FAX 423-576-8424

Nancy Cole
NCC Engineering, Inc.
10518 Raven Court
Knoxville, TN 37922
423-691-8011

Bernard R. Cooper
West Virginia University
Department of Physics
Morgantown, WV 26506-6315
(304) 293-3423
FAX 304-293-3120

Phil Daniel
Babcock & Wilcox
P.O. Box 351
Barberton, OH 44601
(330) 860-1953

R. B. Dooley
EPRI
3412 Hillview Avenue
Palo Alto, CA 94303
(415) 855-2458

John N. DuPont
Lehigh University
Energy Research Center
5 E Packer Avenue
Bethlehem, PA 18015
(610) 758-3942
FAX 610-758-4244

Glen R. Edwards
Colorado School of Mines
Center for Welding, Joining and Coatings Research
Golden, CO 80401-1887
(303) 273-3773
FAX 303-273-3795

Paul Eggerstedt
Industrial Filter and Pump
5900 Ogden Avenue
Cicero, IL 60804
(708) 656-7800
FAX 708-656-7806

William A. Ellingson
Argonne National Laboratory
9700 South Cass Avenue
Bldg. 212
Argonne, IL 60439
(708) 252-5068
FAX 708-252-4798

Jonathan Erpenbach
Oak Ridge National Laboratory
P.O. Box 2008
Oak Ridge, TN 37831-6087
(423) 576-2769

Douglas Fain
East Tennessee Technology Park
P. O. Box 2003
1004-L, MS 7271
Oak Ridge, TN 37831-7271
(423) 574-9932
FAX 423-576-2930

Thomas B. Gibbons
ABB Combustion Engineering
Power Plant Laboratories
2000 Day Hill Road
Windsor, CT 06095
(860) 285-3593

Fred M. Glaser
U.S. Department of Energy
Office of Advanced Research
FE-72
11901 Germantown Road
Germantown, MD 20874
(301) 903-2786
FAX 301-903-8350

G. M. Goodwin
Oak Ridge National Laboratory
P.O. Box 2008
4508, MS 6096
Oak Ridge, TN 37831-6096
(423) 574-4809
FAX 423-574-7721

Howard Halverson
Virginia Polytechnic Institute & State University
Department of Engineering Science and Mechanics
College of Engineering
Blacksburg, VA 24061-0219
(540) 231-7493
FAX 540-231-7187

John Holowczak
United Technologies
Research Center
411 Silver Lane
East Hartford, CT 06108)
FAX 860-610-7879

Linda Horton
Oak Ridge National Laboratory
P. O. Box 2008
4500S, MS 6132
Oak Ridge, TN 37831-6132
(423) 574-5081
FAX 423-574-4066

John P. Hurley
University of North Dakota
Energy & Environmental Research Center
P. O. Box 9018
Grand Forks, ND 58202-9018
(701) 777-5000
FAX 701-777-5181

Carl Irwin
West Virginia University
Department of Physics
P. O. Box 6064
Morgantown, WV 26506-6064
304-293-2867
(FAX) 304-293-3749

Marit Jagtoyen
The University of Kentucky
Center for Applied Energy Research
3572 Iron Works Pike
Lexington, KY 40511-8433
(606) 257-0213

Roger N. Johnson
Pacific Northwest National Laboratory
P. O. Box 999, K3-59
Battelle Boulevard
Richland, WA 99352
(509) 375-6906
FAX 509-375-3864

Roddie R. Judkins
Oak Ridge National Laboratory
P. O. Box 2008
4508, MS 6084
Oak Ridge, TN 37831-6084
(423) 574-4572
FAX 423-574-5812

Matthew June
PALL Corporation
3669 State Route 281
P.O. Box 2030
Cortland, NY 13045
(607-753-6041
FAX 607-753-1220

James Kelly
Rolled Alloys
125 West Sterns Road
P.o. Box 310
Temperance, MI 48182
(313) 847-0561
FAX 313-847-3227

Edgar Lara-Curzio
Oak Ridge National Laboratory
P.O. Box 2008
Oak Ridge, TN 37831-6064
(423) 574-1749
FAX 423-574-6098

Patrick H. Le
Federal Energy Technology Center
3610 Collins Ferry Road
Morgantown, WV 26507-0880
(304) 285-4324
FAX 304-285-4469

Peter Liaw
The University of Tennessee
Department of Materials Science and Engineering
430-C Dougherty Engineering Building
Knoxville, TN 37996-2200
(423) 974-2696
FAX 423-974-4115

C. T. Liu
Oak Ridge National Laboratory
P. O. Box 2008
4500S, MS 6115
Oak Ridge, TN 37831-6115
(423) 574-4459
FAX 423-574-7659

Rick Lowden
Oak Ridge National Laboratory
P. O. Box 2008
4508, MS 6087
Oak Ridge, TN 37831-6087
(423) 576-2769
FAX 423-576-8424

William D. Manly
Oak Ridge National Laboratory
P.O. Box 2008
Oak Ridge, TN 37831-6158
(423) 574-2556
FAX 423-574-5118

Claudette McKamey
Oak Ridge National Laboratory
P. O. Box 2008
4500S, MS 6115
Oak Ridge, TN 37831-6115
(423) 574-6917
FAX 423-574-7659

Theodore McMahon
Federal Energy Technology Center
MS C04
P.O. Box 880
Morgantown, WV 26507-0880
(304) 285-4865
FAX 304-285-4403

Othon Monteiro
Berkeley Laboratory
53-103
1 Cyclotron Road
Berkeley, CA 94720
(510) 486-6159
FAX 510-486-4646

Karren More
Oak Ridge National Laboratory
P.O. Box 2008
Oak Ridge, TN 37831-6064
(423) 574-7788
FAX 423-574-4913

K. Natesan
Argonne National Laboratory
9700 South Cass Avenue
Argonne, IL 60439
(708) 252-5103
FAX 708-252-3604

Dick Nixdorf
REMAXCO Technologies, Inc.
10425 Cogdill Road
Suite 300
Knoxville, TN 37932
(423) 675-1574
FAX 423-675-1581

Parvid Pasto
Oak Ridge National Laboratory
P.O. Box 2008
Oak Ridge, TN 37831-6062
(423) 574-5123
FAX 574-4913

L. R. Pederson
Pacific Northwest National Laboratory
MS K2/44
P. O. Box 999
Richland, WA 99352
(509) 375-2731
FAX 509-375-2186

Kent Probst
Oak Ridge National Laboratory
P.O. Box 2008
Oak Ridge, TN 37831-6063

Robert A. Rapp
Ohio State University
Department of Materials Science and Engineering
116 West 19th Avenue
Columbus, OH 43210-1110
(614) 292-6178
FAX 614-292-1537

Richard B. Read
Federal Energy Technology Center
P. O. Box 10940
Pittsburgh, PA 15236
(412) 892-5721
FAX 412-892-4604

Bill Riley
Albany Research Center
1450 Queen Avenue SW
Albany, OR 97321-2198
(541-967-5851
FAX 541-967-5991

George Roettger
East Tennessee Technology Park
P. O. Box 2003
1004-L, MS 7271
Oak Ridge, TN 37831-7271
(423) 574-7539
FAX 423-576-2930

John Ruether
Federal Energy Technology Center
P.O. Box 10940
Pittsburgh, PA 15236
(412) 892-4832
FAX 412-892-4775

Larry Ruth
Federal Energy Technology Center
P.O. Box 10940
Pittsburgh, PA 15236
(412) 892-4461
FAX 412-892-4822

Vinod K. Sarin
Boston University
College of Engineering
15 St. Mary's Street
Boston, MA 02215
(617) 353-6451
FAX 617-353-5548

Joachim H. Schneibel
Oak Ridge National Laboratory
P.O. Box 2008
Oak Ridge, TN 37831-6115
(423) 576-4644
FAX 423-574-7659

Vinod Sikka
Oak Ridge National Laboratory
P. O. Box 2008
4508, MS 6083
Oak Ridge, TN 37831-6083
(423) 574-5112
FAX 423-4-4357

Prabhu Singh
Westinghouse Electric Corporation
1310 Beulah Road
Pittsburgh, PA 15235-5098
(412) 256-2158
FAX 412-256-2002

Robert Smith
3M Company
Bldg. 203-1-01
3M Center
St. Paul, MN 55144-1000
(612) 733-2564
FAX 612-736-5484

Will Spint
Oak Ridge National Laboratory
P.O. Box 2008
Oak Ridge, TN 37831-6087
(423) 576-2769

Peter Stansberry
Department of Chemical engineering
423 Engineering Sciences Building
P.O. Box 6102
Morgantown, WV 26506-6102
(304) 293-2111, ext. 423
FAX 304-293-4139

Thomas L. Starr
Georgia Institute of Technology
School of Materials Science and
Engineering
Bunger-Henry Building, Room 276
Atlanta, GA 30332-0245
(404) 894-0579
FAX 404-894-9140

David P. Stinton
Oak Ridge National Laboratory
P. O. Box 2008
4515, MS 6063
Oak Ridge, TN 37831-6063
(423) 574-4556
FAX 423-574-4923

N. S. Stoloff
Rensselaer Polytechnic Institute
Materials Engineering Department
Troy, NY 12180-3590
(518) 276-6371
FAX 518-276-8554

Robert W. Swindeman
Oak Ridge National Laboratory
P. O. Box 2008
4500S, MS 6155
Oak Ridge, TN 37831-6155
(423) 574-5108
FAX 423-574-5118

TPeter F. Tortorelli
Oak Ridge National Laboratory
P. O. Box 2008
4500S, MS 6156
Oak Ridge, TN 37831-6156
(423) 574-5119
FAX 423-574-5118

V Srinath Viswanathan
Oak Ridge National Laboratory
P.O. Box 2008
Oak Ridge, TN 37831-6083
(423) 576-9917
FAX 423-574-4357

W Rich Walters
Albany Research Center
1450 Queen Avenue SW
Albany, OR 97321-2198
(541) 967-5873
FAX 541-967-5991

Philip Way
Permeable Ceramics
Ferro Corporation
603 West Commercial St.
E. Rochester, NY 14445
(716) 586-8770
FAX 716-586-7154

Marvis White
U.T. Space Institute
MS-27
B. H. Goethert Parkway
Tullahoma, TN 37388
(615) 393-7502
FAX 615-455-7266

Ian Wright
Oak Ridge National Laboratory
P. O. Box 2008
4500S, MS 6157
Oak Ridge, TN 37831-6157
(423) 574-4451
FAX 423-574-5118

Richard N. Wright
Idaho National Engineering &
Environmental Laboratory
P. O. Box 1625
Idaho Falls, ID 83415-2218
(208) 526-6127
FAX 208-526-0690

Z John Zhu
University of Tennessee
Department of Materials Science and
Engineering
430-C Dougherty Engineering Building
Knoxville, TN 37996-2200
(423) 974-2696
FAX 423-974-4115

CONF-9705115
ORNL/FMP-97/1

INTERNAL DISTRIBUTION

1. K. B. Alexander
2. P. F. Becher
3. B. Bennett
4. T. M. Besmann
5. R. A. Bradley
6. M. Brady
7. K. Breder
8. T. D. Burchell
9. P. T. Carlson
10. J. R. DiStefano
11. J. Erpenbach
12. D. E. Fain
13. G. M. Goodwin
14. J. A. Haynes
15. L. L. Horton
16-19. R. R. Judkins
20. M. A. Karnitz
21. J. R. Keiser
22. E. Lara-Curzio
23. C. T. Liu
24. R. A. Lowden
25. P. J. Maziasz
26. C. G. McKamey
27. K. L. More
28. E. Ohriner
29. A. Pasto
30. B. Pint
31. K. Probst
32. G. E. Roettger
33 G. R. Romanoski
34. A. C. Schaffhauser
35. J. H. Schneibel
36. J. Sheffield
37. V. K. Sikka
38. W. Spint
39. D. P. Stinton
40. R. W. Swindeman
41. T. N. Tiegs
42. P. F. Tortorelli
43. S. Viswanathan
44. D. F. Wilson
45. I. G. Wright
46-47. Central Research Library
48. Document Reference Section
49. ORNL Patent Section
50-51. Laboratory Records Department
52. LRD-RC

EXTERNAL DISTRIBUTION

53. 3M COMPANY, 3M Center, St. Paul, MN 55144
R. G. Smith (Bldg 203-1-01)

54. A. AHLSTROM CORPORATION, Ahlstrom Pyropower, Kanslerinkatu 14, Fin 33720, Tampere, Finland
J. Isaksson

55. ABB Lummus Crest, 15 Broad St., Bloomfield, NJ 07003
M. Greene

56. ABB COMBUSTION ENGINEERING, 911 W. Main St., Chattanooga, TN 37402
D. A. Canonico

57 ABB COMBUSTION ENGINEERING, 2000 Day Hill Road, Windsor, CT 06095
T. B. Gibbons

58. ADIABATICS, INC., 3385 Commerce Dr., Columbus, IN 47201
P. Badgley

59. ADVANCED REFRACTORY TECHNOLOGIES, INC., 699 Hertel Avenue, Buffalo, NY 14207
K. A. Blakely

60. AEA INDUSTRIAL TECHNOLOGY, Harwell Laboratory, Materials Development Division, Bldg. 393, Didcot, Oxfordshire, OX110RA ENGLAND
H. Bishop

61. AIR PRODUCTS AND CHEMICALS, INC., 7201 Hamilton Blvd., Allentown, PA 18195-1501
P. Dyer

62-64. ALBANY RESEARCH CENTER, 1450 Queen Ave., SW, Albany, OR 97321-2198
D. Alman
W. Riley
R. Walters

65. ALBERTA RESEARCH COUNCIL, Oil Sands Research Department, P. O. Box 8330, Postal Station F, Edmonton, Alberta, CANADA T6H5X2
L. G. S. Gray

66. ALLEGHENY LUDLUM STEEL, Technical Center, Alabama and Pacific Avenues, Brackenridge, PA 15014
J. M. Larsen

67. ALLIEDSIGNAL, 2525 W 190th Street, Dept. 93140, Torrance, CA 90504-6099
N. Minh (MS T-41)

68. ALLIEDSIGNAL ENGINES, 111 S. 34th Street, Phoenix, AZ 85071-2181
T. Strangman (MS 553-12)

69. ALLISON ENGINE COMPANY, Materials Engineering, P.O. Box 420, Indianapolis, IN 46206-0420
L. E. Groseclose

70-71 ALLISON GAS TURBINE DIVISION, P. O. Box 420, Indianapolis, IN 46206-0420
P. Khandalwal (Speed Code W-5)
R. A. Wenglarz (Speed Code W-16)

72. ALON PROCESSING, INC., Grantham Street, Tarentum, PA 15084
W. P. Heckel, Jr.

73. ALON PROCESSING, INC., 900 Threadneedle, Vista Bldg, Houston, TX 77079-2990
K. A. Wynns

74. AMAX R&D CENTER, 5950 McIntyre St., Golden, CO 80403
T. B. Cox

75-76. AMERCOM, Advanced Material Division, Atlantic Research Corporation 8928 Fullbright Avenue, Chatsworth, CA 91311
J. O. Bird
W. E. Bustamante

77. AMOCO CHEMICAL COMPANY, P. O. Box 3011, D-2, Naperville, IL 60566-7011
N. Calamur

78. ANSTO, New Illawarra Rd, Lucas Heights NSW 2234 PMB, 1 Menai NSW 2234, Australia
A.B.L. Croker

79. APD INC., 2500 Pearl Buck Road, Bristol, PA 19007
F. Ko

80. A. P. GREEN REFRACTORIES COMPANY, Green Blvd.,
Mexico, MO 65265
J. L. Hill

81-82. ARGONNE NATIONAL LABORATORY, 9700 Cass Ave.,
Argonne, IL 60439
W. A. Ellingson
K. Natesan

83. BABCOCK & WILCOX, P.O. Box 351, Barberton, OH 44601
P. Daniel

84-86. BABCOCK & WILCOX, Lynchburg Research Center, P. O. Box 11165,
Lynchburg, VA 24506
R. Goettler
J. A. Heaney
W. Long

87. BABCOCK & WILCOX INTERNATIONAL, 581 Coronation Blvd.,
Cambridge, Ontario, Canada N1R 5V3
R. Seeley

88. BATTELLE COLUMBUS LABORATORIES, 505 King Ave.,
Columbus, OH 43201
D. Anson

89. BENNETT, Michael J., Three Chimneys, South Moreton Oxon, United Kingdom

90-91. BETHLEHEM STEEL CORPORATION, Homer Research Laboratories,
Bethlehem, PA 18016
B. L. Bramfitt
J. M. Chilton

92. BIRL, 1801 Maple Avenue, Evanston, IL 60201
D. Boss

93. BLACK & VEATCH, 11401 Lamar, Overland Park, KS 66211
M. Bary

94. BOSTON UNIVERSITY, 44 Washington Street, Boston, MA 02215
V. K. Sarin

95. BRITISH COAL CORPORATION, Coal Technology Development Division,
P. O. Box 199, Stoke Orchard, Cheltenham, Glocester,
ENGLAND GL52 4ZG
J. Oakey

96. BROWN UNIVERSITY, Division of Engineering, 182 Hope Street, Providence, RI 02912
K. Kumar

97. CANADA CENTER FOR MINERAL & ENERGY TECHNOLOGY, 568 Booth St., Ottawa, Ontario Canada K1A OG1
R. W. Revie

98. CARR, James P., 15005 Lear Lane, Silver Springs, MD 20905

99. CERAMEM SEPARATIONS, 952 Eat Fir Street, Palmyra, PA 17078
J. Vaklyes, Jr.

100. CHEVRON RESEARCH & TECHNOLOGY COMPANY, 100 Chevron Way, Richmond, CA 94802-0627
D. J. O'Rear

101. CIEMAT, Avda. Complutense, 22, 28040-Madrid (SPAIN)
G. M. Calvo

102. COAL & SYNFUELS TECHNOLOGY, 1616 N. Fort Myer Dr., Suite 1000, Arlington, VA 22209
J. Bourbin

103. COAL TECHNOLOGY CORPORATION, 103 Thomas Road, Bristol, VA 24201
R. A. Wolfe

104. COLORADO SCHOOL OF MINES, Dept. of Metallurgical Engineering, Golden, CO 80401
G. R. Edwards

105. CORNING INCORPORATED, SP-D V-1-9, Corning, NY 14831
P. Bardhan

106. DB Riley, Inc., 45 McKeon Road, Worcester, MA 01610
G. S. Gielda

107. DEVASCO INTERNATIONAL, INC., 9618 W. Tidwell, Houston, TX 77041
J. L. Scott

108. J. DOWICKI, P.E., 19401 Framingham Dr., Gaithersburg, MD 20879

109. DUPONT LANXIDE COMPOSITES, INC., Pencader Plant, Box 6100, Newark, DE 19714-6100
J. K. Weddell

110-111. DUPONT LANXIDE COMPOSITES, INC., 1300 Marrows Road,
P.O. Box 6077, Newark, DE 19714-6077
A. Z. Fresco
D. Landini

112. EC TECHNOLOGIES, INC., 3614 Highpoint Dr.,
San Antonio, TX 78217
D. J. Kenton

113. EG&G IDAHO, INC., Idaho National Engineering & Environmental Laboratory,
P.O. Box 1625, Idaho Falls, ID 83415
R. N. Wright

114-116. ELECTRIC POWER RESEARCH INSTITUTE, P.O. Box 10412,
3412 Hillview Avenue, Palo Alto, CA 94303
W. T. Bakker
R. B. Dooley
J. Stringer

117. ELECTRO PHYSICS, INC., 1400 Marshall Street, NE,
Minneapolis, MN 55413
D. Bell

118. ENERGY AND WATER RESEARCH CENTER, P. O. Box 6064
West Virginia University,
Morgantown, WV 26505-5054
P. G. Stansberry

119. ENVIRONMENTAL PROTECTION AGENCY, Global Warming Control
Division (MD-63), Research Triangle Park, NC 27711
K. T. Janes

120. ERC, INC., P. O. Box 417, Tullahoma, TN 37388
Y. C. L. Susan Wu

121-122. EXXON RESEARCH AND ENGINEERING COMPANY, Clinton Township,
Route 2 East, Annandale, NJ 08801
M. L. Gorbaty
S. Soled

123. FERRO CORPORATION, Permeable Ceramics, 603 West Commercial St.
E., Rochester, NY 14445
P. S. Way

124. FORSCHUUGS ZENTRUM JÜLICH GmbH, ICT, Postfach 1913, D-5170
Jülich, Germany
H. Barnert-Wiemer

125. FOSTER WHEELER DEVELOPMENT CORPORATION, Materials Technology Dept., John Blizard Research Center, 12 Peach Tree Hill Road, Livingston, NJ 07039
J. L. Blough

126. FRAUNHOFER-INSTITUT für WERKSTOFFMECHANIK, Wohlerstrass 11, 79108 Freiburg, West Germany
R. Westerheide

127. GAS RESEARCH INSTITUTE, 8600 West Bryn Mawr Avenue, Chicago, IL 60631
H. S. Meyer

128. GENERAL APPLIED SCIENCE LABS, 77 Raynor Avenue, Ronkonkoma, NY 11779
M. Novack

129. GENERAL ELECTRIC CORPORATE CR&D, P.O. Box 8, Bldg. K1, MB 265, Schenectady, NY 12301
G. Rowe

130. GEORGIA INSTITUTE OF TECHNOLOGY, Georgia Tech Research Institute, 123D Baker Bldg., Atlanta, GA 30332-0245
T. L. Starr

131. GRI, 8600 W. Bryn Mawr, Chicago, IL 60656
D. Scarpiello

132. HAYNES INTERNATIONAL, INC., 1020 W. Park Avenue, Kokomo, IN 46904
M. Harper

133. HOSKINS MANUFACTURING COMPANY, 10776 Hall Rd., Hamburg, MI 48139-0218
F. B. Hall

134. ILLINOIS INSTITUTE OF TECHNOLOGY, METM Dept., Perlstein Hall, IIT, Chicago, IL 60616
J. A. Todd-Copley

135. INCO ALLOYS INTERNATIONAL, INC., P. O. Box 1958, Huntington, WV 25720
S. Tassen

136. INDUSTRIAL FILTER & PUMP, 5900 Ogden Avenue, Cicero, IL 60804
P. Eggerstedt

137. INTECH, INC., 11316 Roven Dr., Potomac, MD 20854-3126
P. Lowe

138-139. IOWA STATE UNIVERSITY, Ames Laboratory, 107 Metals Development, Ames, IA 50011
D. J. Sordelet
Ozer Unal

140. JET PROPULSION LABORATORY, 4800 Oak Grove Dr., MS-79-21, Pasadena, CA 91020
R. L. Chen

141. LANXIDE CORPORATION, 1 Tralee Industrial Park, Newark, DE 19711
E. M. Anderson

142. LAVA CRUCIBLE-REFRACTORIES CO., P.O. Box 278, Zelienople, PA 16063
T. Mulholland

143-144. LAWRENCE BERKELEY LABORATORY, University of California, 1 Cyclotron Road, Berkeley, CA 94720
I. Brown - MS 53
O. Monteiro - 53-103

145. LAWRENCE LIVERMORE NATIONAL LABORATORY, P.O. Box 808, Livermore, CA 94551
J. H. Richardson (L-353)

146-147. LEHIGH UNIVERSITY, Energy Research Center, 5 E Packer Avenue, Bethlehem, PA 18015
S. W. Banovic
J. N. DuPont

148. LIQUID CARBONIC INDUSTRIAS S.A, Avenida Rio Branco, 57-6° Andar, Centro - 20090-004, Rio De Janeiro, Brazil
M. Saddy

149. LOCKHEED MARTIN-KAPL, P.O. Box 1072, MS G2-312, Schenectady, NY 12301
J. J. Letko (MS D2-121)

150. E. LORIA, 1829 Taper Drive, Pittsburgh, PA 15241

151. LOS ALAMOS NATIONAL LABORATORY, P.O. Box 1663, Los Alamos, NM 87545
R. G. Castro - MS G720

152. LURGI LENTJES BABCOCK, Duisburger Strasse 375, D-46041 Oberhausen, Germany
G. von Wedel

153-154. MALLETT TECHNOLOGY, 100 Park Drive, Suite 204, P.O. Box 14407, Research Triangle Park, NC 27709
R. Mallett
J. L. Bitner

155. MASSACHUSETTS INSTITUTE OF TECHNOLOGY, Department of Chemical Engineering, Room 66-456, Cambridge, MA 02139
J. Longwell

156. MICROCOATING TECHNOLOGIES, 430 Tenth St., NW, Suite N-108, Atlanta, GA 30318-5769
S. Shanmugham

157. MOBIL RESEARCH & DEVELOPMENT CORPORATION, P. O. Box 1026, Princeton, NJ 08540
R. E. Searles

158. NASA LEWIS RESEARCH CENTER, 21000 Brookpark Road, Cleveland, OH 44135
N. Jacobson - MS 106-1

159. NATIONAL INSTITUTE OF STANDARDS AND TECHNOLOGY, Materials Building, Gaithersburg, MD 20899
L. K. Ives (Bldg. 220, Rm. A-215)

160. NATURAL GAS AND OIL TECHNOLOGY PARTNERSHIP, 12434 Penthshire, Houston, TX 77024
R. M. Whitsett

161. NETHERLANDS ENERGY RESEARCH FOUNDATION ECN, P.O. Box 1, 1755 ZG Petten, The Netherlands
P. T. Alderliesten

162. NEW ENERGY AND INDUSTRIAL TECHNOLOGY DEVELOPMENT ORGANIZATION, 1800 K Street, N.W., Suite 924, Washington, DC 20006
T. Fukumizu

163-165. NEW ENERGY AND INDUSTRIAL TECHNOLOGY DEVELOPMENT ORGANIZATION, Sunshine 60 Bldg., P.O. Box 1151, 1-1 Higashi-Ikebukuro 3-Chome, Toshima-Ku, Tokyo, 170, Japan
S. Hirano
H. Narita
S. Ueda

166. NORCONTROL, Duran Marquina 20, 15080 La Coruna, Spain
S. Gomez

167. OFFICE OF NAVAL RESEARCH, Code 431, 800 N. Quincy St., Arlington, VA 22217
S. G. Fishman

168. OHIO STATE UNIVERSITY, Department of Metallurgical Engineering, 116 W. 19th Avenue, Columbus, OH 43210
R. A. Rapp

169-170. PACIFIC NORTHWEST NATIONAL LABORATORIES, P.O. Box 999, Richland, WA 99352
R. N. Johnson
L. R. Pederson

171. PALL CORPORATION, 3669 State Route 281, P.O. Box 2030, Cortland, NY 13045
M. June

172. PENNSYLVANIA STATE UNIVERSITY, 101 Steidle Building, University Park, PA 16802
R. Tressler

173. PSI TECHNOLOGY COMPANY, 20 New England Business Center, Andover, MA 01810
L. Bool

174. REMAXCO TECHNOLOGIES, INC., 10425 Cogdill Road, Suite 300 Knoxville, TN 37932
D. Nixdorf

175. RENSSELAER POLYTECHNIC INSTITUTE, Materials Engineering Department, Troy, NY 12180-3590
N. S. Stoloff

176. RIBBON TECHNOLOGY CORPORATION, P.O. Box 30758, Columbus, OH 43230
T. Gaspar

177. RISO NATIONAL LABORATORY, P.O. Box 49, DK-4000, Roskilde, DENMARK
Aksel Olsen

178. ROLLED ALLOYS, 125 West Sterns Road, Temperance, MI 48182
J. C. Kelly

179. SANDIA NATIONAL LABORATORIES, 7011 East Avenue, P.O. Box 969
Livermore, CA 94551-0969
J. E. Smugeresky (MS-9402)

180. SANDIA NATIONAL LABORATORIES, P.O. Box 5800,
Albuquerque, NM 87185
G. Carlson

181-182. SARGENT AND LUNDY, 55 E Monroe Street, Chicago, IL 60603
R. J. Kerhin
D. G. Sloat

183. SCIENCE APPLICATIONS INTERNATIONAL CORPORATION,
1710 Goodridge Dr., McLean, VA 22102
J. T. Bartis

184. SFA PACIFIC, INC., 444 Castro Street, Suite 920, Mountain View, CA 94041
N. Korens

185. SHELL DEVELOPMENT COMPANY, P.O. Box 1380,
Houston, TX 77251-1380
L. W. R. Dicks

186. G. SORELL, 49 Brookside Terrace, N. Caldwell, NJ 07006

187. SOUTHERN RESEARCH INSTITUTE, 2000 Ninth Avenue South,
Birmingham, AL 35202
H. S. Starrett

188. SOUTHWEST RESEARCH INSTITUTE, 6620 Culebra Road,
P.O. Drawer 28510, San Antonio, TX 78284
F. F. Lyle, Jr.

189. SRI INTERNATIONAL, 333 Ravenswood Avenue, Meno Park, CA 04025
Y. D. Blum

190. STANTON ENERGY INDUSTRY CONSULTANTS, INC., RD #1,
Liberty Court,
New Stanton, PA 15672-9621
R. J. Steffen

191. SUNDSTRAND, 4747 Harrison Ave., Rockford, IL 61125
D. Oakey

192. SUPERKINETICS, 2881 Tramway Place, NE,
Albuquerque, NM 87122
J. V. Milewski

193. TECHNIWEAVE, INC., 109 Chestnut Hill Road, Rochester, NH 03868
J. A. LeCoustaouec

194. TECHNOLOGY MANAGEMENT INC., 9718 Lake Shore Blvd., Cleveland, OH 44108
B. P. Lee

195. TELEDYNE ALLVAC, P.O. Box 5030, Monroe, NC 28110
A. L. Coffey

196-197. TENNESSEE VALLEY AUTHORITY, 3N66A Missionary Ridge Place, Chattanooga, TN 37402-2801
J. B. Brooks
C. M. Huang

198. TEXAS EASTERN TRANSMISSION CORPORATION, P.O. Box 2521, Houston, TX 77252
D. H. France

199. THE AMERICAN CERAMIC SOCIETY, INC., 735 Ceramic Place, Westerville, OH 43081
L. Sheppard

200. THE JOHNS HOPKINS UNIVERSITY, Materials Science & Engineering, Maryland Hall, Baltimore, MD 21218
R. E. Green, Jr.

201. THE MATERIALS PROPERTIES COUNCIL, INC., United Engineering Center, 345 E. Forty-Seventh St., New York, NY 10017
M. Prager

202. THE NORTON COMPANY, High Performance Ceramics Division, Goddard Road, Northboro, MA 01532-1545
N. Corbin

203. THE RALPH M. PARSONS COMPANY, 100 West Walnut St., Pasadena, CA 91124
J. B. O'Hara

204. THE TORRINGTON COMPANY, Advanced Technology Center, 59 Field Street, Torrington, CT 06790
W. J. Chmura

205. TRW, 1455 E. 195th Street, Cleveland, OH 44110
M. Kurup

206-207. UNITED TECHNOLOGIES RESEARCH CENTER, Materials Department, 411 Silver Lane, East Hartford, CT 06108
N. S. Bornstein
J. E. Holowczak

208. UNIVERSITY OF CALGARY, 2500 University Dr. NW, Calgary, Canada
S. X. Mao

209. UNIVERSITY OF CALIFORNIA, Department of Materials Science and Mineral Engineering, University of California, Building 66-Room 247, Berkeley, CA 94720
R. O. Richie

210-211. UNIVERSITY OF KENTUCKY, Center for Applied Energy Research, 3572 Iron Works Pike, Lexington, KY 40511-8433
F. Derbyshire
M. Jagtoyen

212. UNIVERSITY OF NORTH DAKOTA, P.O. Box 9018, University Station, Grand Forks, ND 58202
J. P. Hurley

213. UNIVERSITY OF PITTSBURGH, Materials Science & Engineering Department, 848 Brenedum Hall, Pittsburgh, PA 15261
N. Birks

214. UNIVERSITY OF SOUTH AUSTRALIA, Department of Metallurgy, The Levels SA 5095 Australia
K. N. Strafford

215-217. UNIVERSITY OF TENNESSEE, Department of Materials Science and Engineering, 434 Doughtery Engineering Building, Knoxville, TN 37996
R. A. Buchanan
P. Liaw
C. D. Lundin

218. UNIVERSITY OF TENNESSEE SPACE INSTITUTE, Tullahoma, TN 37388
M. White

219. UNIVERSITY OF WASHINGTON, Department of Materials Science and Engineering, 101 Wilson, FB-10, Seattle, WA 98195
T. G. Stoebe

220. UNIVERSITY OF WISCONSIN, Department of Materials Science and Engineering, 1509 University Avenue, Madison, WI 53706-1595
J. H. Perepezko

221. UOP, 50 E. Algonquin Road, Des Plaines, IL 60017-5016
G. J. Antos

222. VEBA OEL, P. O. Box 45, 4650 Gelsenkirchen-Buer, Germany
D. Fuhrmann

223-224. VIRGINIA POLYTECHNIC INSTITUTE AND STATE UNIVERSITY, Department of Materials Engineering, Blacksburg, VA 24061
W. Curtin
K. L. Reifsnyder

225. WESSEL, James K.,127 Westview Lane, Oak Ridge, TN 37830

226-228. WEST VIRGINIA UNIVERSITY, Mechanical & Aerospace Engineering Department, P.O. Box 6106, Morgantown, WV 26505
B. Cooper
B. Kang
P. Stansberry

229. WESTERN RESEARCH INSTITUTE, 365 N. 9th Street, P. O. Box 3395, University Station, Laramie, WY 82071
V. K. Sethi

230. WESTINGHOUSE ELECTRIC CORPORATION, 4400 Alafaya Trial, Orlando, FL 32826-2399
S. M. Sabol - MC 303

231-233. WESTINGHOUSE ELECTRIC CORPORATION, Research and Development Center, 1310 Beulah Road, Pittsburgh, PA 15235-5098
M. A. Alvin
G. Bruck
P. Singh

234. WORCESTER POLYTECHNIC INSTITUTE, 100 Institute Road, Worcester, MA 01609
E. Ma

235. DOE CHICAGO OPERATIONS OFFICE, 9800 S. Cass Ave., Argonne, IL 60439
J. Jonkouski

236. DOE IDAHO OPERATIONS OFFICE, 765 DOE Place, Idaho Falls, ID 83406
J. B. Malmo

237-251. DOE FEDERAL ENERGY TECHNOLOGY CENTER,
P.O. Box 880, Morgantown, W VA 26505
C. T. Alsup
R. A. Bajura
R. C. Bedick
D. C. Cicero
F. W. Crouse, Jr.
R. A. Dennis
U. Grimm
J. S. Halow
N. T. Holcombe
W. J. Huber
P. Lee
T. J. McMahon
H. M. Ness
J. E. Notestein
C. M. Zeh

252. DOE OAK RIDGE OPERATIONS OFFICE, Oak Ridge, P. O. Box 2008,
Oak Ridge, TN 37831-6269
M. A. Rawlins

253. DOE OFFICE OF BASIC ENERGY SCIENCES, Materials Sciences Division,
ER-131, 19901 Germantown Road, Germantown, MD 20874-1290
J. N. Mundy

254. DOE OFFICE OF ENERGY EFFICIENCY AND RENEWABLE ENERGY,
CE-12, Forrestal Building, Washington, DC 20545
J. J. Eberhardt

255-256. DOE OFFICE OF ENERGY RESEARCH, 14 Goshen Court,
Gaithersburg, MD 20882-1016
N. F. Barr
F. J. Wobber

257-262. DOE OFFICE OF FOSSIL ENERGY, Washington, DC 20585
H. Feibus (FE-23)
K. N. Frye (FE-13)
F. M. Glaser (FE-72)
S. C. Jain (FE-231)
T. B. Simpson (FE-231)
M. I. Singer (FE-70)

263. DOE OFFICE OF INDUSTRIAL TECHNOLOGIES, 1000 Independence Avenue
S.W., Washington, DC 20585
S. Dillich (EE-20)

264. DOE OFFICE OF NAVAL REACTORS, NE-60, Crystal City Bldg., N.C.-2, Washington, DC 20585
J. Mosquera

265. DOE OFFICE OF PETROLEUM RESERVES, Analysis Division, FE-431, 1000 Independence Ave., Washington, DC 20585
D. de B. Gray

266-279. DOE FEDERAL ENERGY TECHNOLOGY CENTER, P. O. Box 10940, Pittsburgh, PA 15236
A. H. Baldwin
J. L. Balzarini
R. A. Carabetta
R. C. Dolence
P. Goldberg
J. D. Hickerson
J. J. Lacey
S. R. Lee
M. E. Mather
G. V. McGurl
J. A. Ruether
L. Ruth
T. M. Torkos

280-281. DOE, OFFICE OF SCIENTIFIC AND TECHNICAL INFORMATION, P.O.Box 62, Oak Ridge, TN 37831

For distribution by microfiche as shown in DOE/OSTI-4500,
Distribution Category UC-114 (Coal Based Materials and Components)